AD 732511

DEPARTMENT OF THE NAVY
NAVAL SHIP RESEARCH AND DEVELOPMENT CENTER
WASHINGTON, D.C. 20034

DESIGN, CAVITATION PERFORMANCE, AND OPEN-WATER PERFORMANCE OF A SERIES OF RESEARCH SKEWED PROPELLERS

by

Robert J. Boswell

March 1971

Report 3339

UNCLASSIFIED

Security Classification

DOCUMENT CONTROL DATA - R & D

(Security classification of title, body of abstract and indexing annotation must be entered when the overall report is classified)

1. ORIGINATING ACTIVITY (Corporate author) Naval Ship Research and Development Center Washington, D.C. 20034	2a. REPORT SECURITY CLASSIFICATION UNCLASSIFIED
	2b. GROUP

3. REPORT TITLE

DESIGN, CAVITATION PERFORMANCE, AND OPEN-WATER PERFORMANCE OF A SERIES OF RESEARCH SKEWED PROPELLERS

4. DESCRIPTIVE NOTES (Type of report and inclusive dates)

5. AUTHOR(S) (First name, middle initial, last name)

Robert J. Boswell

6. REPORT DATE	7a. TOTAL NO. OF PAGES	7b. NO. OF REFS
March 1971	44	14

8a. CONTRACT OR GRANT NO.	9a. ORIGINATOR'S REPORT NUMBER(S) Report 3339
b. PROJECT NO.	
c. Subproject ZR011-0101	9b. OTHER REPORT NO(S) (Any other numbers that may be assigned this report)
d.	

10. DISTRIBUTION STATEMENT

Approved for Public Release: Distribution Unlimited

11. SUPPLEMENTARY NOTES	12. SPONSORING MILITARY ACTIVITY
Most of the work reported was supported by: Maritime Administration, Pacific Far East Lines, Prudential Lines, Inc., & Friede and Goldman, Inc.	NSRDC IR/IED Program Washington D.C. 20034

13. ABSTRACT

Cavitation tunnel and open-water results are presented for a series of skewed propellers that were designed by lifting-surface methods. The four model propellers had maximum projected skew at the blade tip equal to 0, 36, 72, and 108 deg. The results showed that the cavitation-free bucket becomes substantially wider with increasing skew: however, there was some crossover in the inception of back cavitation and tip vortex cavitation among the three skewed designs near design advance coefficient. Near the self-propulsion condition, the propeller with 36 deg of skew had the highest cavitation inception speed. Forward open-water propulsion performance including lift effectiveness and performance breakdown due to cavitation were substantially the same for the four propellers. All four propellers developed the design thrust loading coefficient within 1 percent of design rpm in open water. At constant power and thrust loading coefficients, the backing speed decreased slightly with increasing skew (respective reductions of 1.5, 8.0, and 12.5 percent for 36, 72, and 108 deg of skew).

DD FORM 1 NOV 65 1473 (PAGE 1)

S/N 0101-807-6801

UNCLASSIFIED

Security Classification

14 KEY WORDS	LINK A		LINK B		LINK C	
	ROLE	WT	ROLE	WT	ROLE	WT
Propellers						
Skewed Propellers						
Cavitation						
Cavitation Inception						
Model Tests						
Lifting Surface Design						
Subcavitating Propeller						
Propeller Backing						

TABLE OF CONTENTS

LIST OF FIGURES

LIST OF TABLES

NOTATION

A_0	Disk area of propeller, πR^2
C_p	Power coefficient, $C_p = 2\pi nQ / \frac{\rho}{2} A_0 V_A^3$
C_{T_h}	Thrust loadin~ coefficient, $C_{T_h} = T / \frac{\rho}{2} A_0 V_A^2$
c	Section chord length
D	Propeller diameter
f_M	Section camber
g	Acceleration due to gravity
H	Hydrostatic head at shaft centerline minus vapor pressure
$IVFV$	Inception of face vortex cavitation
$IVTV$	Inception of tip vortex cavitation
J	Advance coefficient, $J = V_A / nD$
K_Q	Torque coefficient, $K_Q = Q / \rho n^2 D^5$
K_T	Thrust coefficient, $K_T = T / \rho n^2 D^4$
n	Propeller revolutions per unit time, positive forward
P	Propeller section pitch
P_D	Power delivered to the propeller
Q	Propeller torque, positive in direction rotating propeller forward
R	Propeller radius
$R_{n_{0.7}}$	Reynolds number at 0.7 R, $R_{n_{0.7}} = \dfrac{c_{0.7}\sqrt{V_A^2 + (0.7\pi nD)^2}}{\nu}$
r	Radial distance from propeller axis
T	Propeller thrust, positive in direction propelling ship forward
t	Maximum thickness of propeller blade section
V_A	Speed of advance of propeller, positive forward
V_s	Ship speed

x	Nondimensional radius, $x = r/R$
Z	Number of blades
β_i	Hydrodynamic pitch angle
θ_s	Projected skew angle at radius r
η_0	Propeller open-water efficiency, $\eta_0 = J/2\pi \cdot K_T / K_Q$
ν	Kinematic viscosity of water
ρ	Density of water
σ	Cavitation number based on vapor pressure, $\sigma = 2gH/V_A^2$

ABSTRACT

Cavitation tunnel and open-water results are presented for a series of skewed propellers that were designed by lifting-surface methods. The four model propellers had maximum projected skew at the blade tip equal to 0, 36, 72, and 108 deg. The results showed that the cavitation-free bucket becomes substantially wider with increasing skew; however, there was some crossover in the inception of back cavitation and tip vortex cavitation among the three skewed designs near design advance coefficient. Near the self-propulsion condition, the propeller with 36 deg of skew had the highest cavitation inception speed. Forward open-water propulsion performance including lift effectiveness and performance breakdown due to cavitation were substantially the same for the four propellers. All four propellers developed the design thrust loading coefficient within 1 percent of design rpm in open water. At constant power and thrust loading coefficients, the backing speed decreased slightly with increasing skew (respective reductions of 1.5, 8.0, and 12.5 percent for 36, 72, and 108 deg of skew).

ADMINISTRATIVE INFORMATION

The work reported herein was conducted in 1968. Financial support was furnished mainly by the Maritime Administration, Pacific Far East Lines, Prudential Lines, Inc., and Friede and Goldman, Inc. Friede and Goldman, Inc. administered the funding under the development program for the LASH Cargo vessels. The backing tests were performed under the in-house independent research program of the Naval Ship Research and Development Center (NSRDC) and funded under Subproject ZR011-0101.

INTRODUCTION

Interest in highly skewed propellers for surface ships was stimulated by a previous NSRDC investigation with a highly skewed research model propeller. That investigation indicated appreciable benefits from the use of blade skew, e.g., substantial reductions in propeller force and moment fluctuations[1] and improved tolerance to the inception of cavitation caused by fluctuations in angle of attack due to operation in a wake.[2] Since there was no deterioration in propulsion characteristics, i.e., efficiency and thrust and torque breakdown due to cavitation, it appeared feasible to consider the use of propeller blade skew as a method of improving propeller cavitation erosion and vibration characteristics without handicapping powering performance. In view of the limited knowledge regarding the effects of various

---

[1]References are listed on page 34.

amounts of skew, however, a parametric study was considered necessary prior to making any definite performance and cavitation predictions for skewed propellers.

In this subsequent parametric study, a series of four propellers was designed, built to model scale, and tested. This report presents the design, open-water performance, and cavitation performance of these propellers. In another phase of the systematic study of skew, these model propellers were used to investigate the effect of skew on unsteady propeller bearing forces and moments due to operation in a nonuniform flow field and propeller-induced pressures.[4] A summary of all these results was presented by Cox and Boswell.

Except as previously noted,[2] no data were found in the literature on the effect of skew on cavitation. Shiba[6] speculated that skew would delay the inception of cavitation, but he presented no data to substantiate his speculation. Delano and Harrison[7] experimentally observed that large amounts of skew on aircraft propellers delay the onset of adverse compressibility effects, which may be analogous to the cavitation effects on marine propellers.

PROPELLER DESIGNS

Four propellers were designed using the lifting-surface procedure of Cheng[8] together with thickness corrections of Kerwin and Leopold.[9] The conditions for which these propellers were designed are typical of container ships or single-screw destroyer-type ships. The four propellers had five blades and maximum skew angles (measured in the plane of the propeller disk) of 0, 36, 72, and 108 deg. These angles correspond to 0, 0.5, 1.0, and 1.5 times the blade angular spacing. All parameters except skew (and pitch and camber corrections due to skew) were held constant for the four designs.

It is emphasized that the pitch correction due to skew is very substantial and that a skewed propeller with the desired radial distribution of loading can be designed only by the use of lifting-surface techniques. To the writer's knowledge, these propellers are the first model marine propellers so designed to methodically investigate the effects of skew.

Blade stress was calculated by beam theory. The effect of skew on the stress due to centrifugal forces was calculated using the method outlined by Schoenherr.[10] The calculated stress level increased moderately with skew. The radial thickness distribution and blade outline (identical for all propellers) was selected such that the geometry and calculated stress of the propellers with 0, 36, and 72 deg of skew complied with requirements specified by the American Bureau of Shipping,[11] i.e., maximum working stress of 9000 psi for manganese-nickel-aluminum-bronze (superston 40 - grade 5). However, it was not clear whether the beam theory adequately predicts the stress in highly skewed propellers. Accordingly, the steady stress of a highly skewed propeller blade was investigated experimentally at NSRDC[12] (after the designs of the propellers reported herein were completed). These results indicate that full-scale prototypes of the propellers with 0, 36, and 72 deg of skew should possess adequate strength from the point of view of steady stress. However the effect of skew on unsteady stress is not known. Since the existing strength data are very limited, NSRDC plans additional experimental and theoretical work on the effect of skew on blade stress.

The principal design characteristics of the propellers are shown in Table 1 and outline drawings of the propeller blades are given in Figure 1. Figure 2 is a photograph of the four propellers.

TABLE 1

Geometry of Propellers

Number of Blades	5
Expanded Area Ratio	0.725
Section Meanline	NACA $a = 0.8$
Section Thickness Distribution	NACA 66 with NSRDC modified nose and tail
Design J	0.889
Design C_{T_h}	0.534

r/R	$\tan\beta_i$	c/D	t/C
0.2	1.8256	0.174	0.2494
0.3	1.3094	0.229	0.1562
0.4	1.0075	0.275	0.1068
0.5	0.8034	0.312	0.0768
0.6	0.6483	0.337	0.0566
0.7	0.5300	0.347	0.0421
0.8	0.4390	0.334	0.0314
0.9	0.3681	0.280	0.0239

Propeller 4381 (Skew = 0 Deg)

r/R	θ_s (deg)	P/D	f_M/c
0.3	0.0	1.3448	0.0368
0.4	0.0	1.3580	0.0348
0.5	0.0	1.3361	0.0307
0.6	0.0	1.2797	0.0245
0.7	0.0	1.2099	0.0191
0.8	0.0	1.1366	0.0148
0.9	0.0	1.0660	0.0123

TABLE 1 (Continued)

Propeller 4382 (Skew = 36 Deg)

r/R	θ_s (deg)	P/D	f_M/c
0.3	4.655	1.4332	0.0370
0.4	9.363	1.4117	0.0344
0.5	13.948	1.3613	0.0305
0.6	18.378	1.2854	0.0247
0.7	22.747	1.1999	0.0199
0.8	27.145	1.1117	0.0161
0.9	31.575	1.0270	0.0134

Propeller 4383 (Skew = 72 Deg)

r/R	θ_s (deg)	P/D	f_M/c
0.3	9.293	1.5124	0.0407
0.4	18.816	1.4588	0.0385
0.5	27.991	1.3860	0.0342
0.6	36.770	1.2958	0.0281
0.7	45.453	1.1976	0.0230
0.8	54.245	1.0959	0.0189
0.9	63.102	0.9955	0.0159

Propeller 4384 (Skew = 108 Deg)

r/R	θ_s (deg)	P/D	f_M/c
0.3	13.921	1.5837	0.0479
0.4	28.426	1.4956	0.0453
0.5	42.152	1.4057	0.0401
0.6	55.199	1.3051	0.0334
0.7	68.098	1.1993	0.0278
0.8	81.283	1.0864	0.0232
0.9	94.624	0.9729	0.0193

TEST PROCEDURE

Open-water propulsion tests of the four 1-ft-diameter model propellers were conducted in the NSRDC deep-water basin; the propeller boat was instrumented with a gravity dynamometer for the forward tests and with a transmission dynamometer for the backing tests. The forward tests for all propellers were run at 7.8 rps and at speed of advance V_A varying from 3.0 to 10.0 ft/sec, permitting operation at a Reynolds number $R_{n_{0.7}}$ from 6.1×10^5 to 6.9×10^5. The backing tests for all propellers were run at -8.33 rps and at V_A varying from -3.0 to -9.5 ft/sec, permitting operation at $R_{n_{0.7}}$ from 6.4×10^5 to 7.4×10^5.

The cavitation tests were conducted in the NSRDC 24-in. variable-pressure water tunnel in uniform flow using the open-jet test section and a downstream shaft driven by a 150-hp dynamometer. Each propeller was tested over a range of advance coefficient J and cavitation number σ. For each advance coefficient, the tunnel water speed was calibrated by setting thrust and rps based on the open-water test for the propeller. At each advance coefficient, the cavitation test was conducted by starting from a noncavitating condition and reducing the tunnel pressure (and thus σ) until cavitation appeared and/or until the cavitation pattern changed significantly. The cavitation patterns at these pressures were photographed and sketched, and the propeller thrust and torque recorded. The cavitation tests for all propellers were run at $n = 14$ to 20 rps and $V_A = 10$ to 20 ft/sec, i.e., $R_{n_{0.7}} = 1.38 \times 10^6$ to 2.44×10^6. The total air content, as measured with a Van-Slyke apparatus, was maintained at 25 to 30 percent of saturation at atmospheric pressure.

TEST RESULTS

Figure 3 presents the forward open-water propulsion characteristics of the four propellers. The variation of the open-water propulsion characteristics with skew was negligible. Not only was the performance of the four propellers essentially the same at design condition, but the lift effectiveness (slope of the curve of thrust coefficient K_T versus advance coefficient J) was substantially independent of skew. A comparison of experimental performance with design conditions (Tables 2 and 3) revealed that all the propellers operated within 1 percent of design rpm. All the variations between design and experiment were within manufacturing tolerance and experimental accuracy. The uniformly good agreement for all values of skew confirmed the design technique for highly skewed propellers.

Figure 4 presents the backing open-water performance of the four propellers. Table 4 shows the effect of skew on steady backing speed at constant power and constant thrust loading coefficient. These tables were computed by entering the backing open-water curves at constant values of thrust loading coefficient, $C_{T_h} = 8K_T / \pi J^2$. At the corresponding advance coefficient J, the power coefficient $C_p = 2\pi nQ / \frac{1}{2}\rho V_A^3 A_0 = 16K_Q / J^3$ was obtained from the open-water curves. Constant power, $P_D = 2\pi nQ$, and diameter were specified; therefore the speed of advance for each propeller was $V_A = (P_D / \frac{1}{2}\rho C_p A_0)^{1/3}$. These data show that backing speed decreased slightly with increasing skew and that the amount of reduction was insensitive to the thrust loading coefficient in the region $C_{T_h} = 0.2$ to 1.6. The backing speed with 36, 72, and 108 deg of skew were approximately 1.5, 8.0, and 12.5 percent less respectively than the backing speed with zero skew.

TABLE 2

Forward Open-Water Performance at Design Advance Coefficient

($J = 0.889$)

Propeller		Design	Open Water	Percent Difference
4381	K_T	0.213	0.208	−2.3
	$10\,K_Q$	0.447	0.445	−0.4
	η_0	0.673	0.661	−1.8
4382	K_T	0.213	0.205	−3.8
	$10\,K_Q$	0.447	0.440	−1.6
	η_0	0.673	0.657	−2.4
4383	K_T	0.213	0.214	+0.5
	$10\,K_Q$	0.447	0.460	+2.9
	η_0	0.673	0.658	−2.2
4384	K_T	0.213	0.208	−2.3
	$10\,K_Q$	0.447	0.446	−0.2
	η_0	0.673	0.660	−1.9

TABLE 3

Forward Open-Water Performance at Design Thrust Loading Coefficient

(Design conditions: $C_{T_h} = 0.534$ and $J = 0.889$)

Propeller	Experimental J at Design C_{T_h}	Percent Difference
4381	0.884	−0.6
4382	0.881	−1.0
4383	0.890	+0.1
4384	0.883	−0.7

TABLE 4

Effect of Skew on Steady Backing Speed at Constant Power

C_{T_h}	$\frac{V_A \text{ (Skew = 36 deg)}}{V_A \text{ (Skew = 0 deg)}}$	$\frac{V_A \text{ (Skew = 72 deg)}}{V_A \text{ (Skew = 0 deg)}}$	$\frac{V_A \text{ (Skew = 108 deg)}}{V_A \text{ (Skew = 0 deg)}}$
0.2	0.983	0.898	0.871
0.4	0.990	0.917	0.884
0.8	0.993	0.921	0.885
1.2	0.987	0.920	0.877
1.6	0.984	0.918	0.871

Figures 5a–5d show cavitation inception for the four propellers at various radii, and Figure 6 compares the inception on the different propellers. Sketches and photographs of the cavitation at selected advance coefficients and cavitation numbers are given in Figures 7a–7e. In general, the sheet cavitation on both back and face started near the tip and proceeded to lower radii with decreasing cavitation number. On the two most highly skewed propellers, back cavitation started near the tip and, at lower cavitation numbers, a separate cavity formed at inner radii.

On Figures 5a – 5d, a curve marked with one radius means that the propeller was cavitating from that radius to the tip. Curves showing the inception of the separate inner cavity are marked with the radial extent of the inner cavity.

The leading-edge face cavitation for the skewed propellers appears to be like a cavitating vortex parallel to the leading edge and slightly removed from the blade surface (see Figure 7e). Back bubble cavitation started at essentially the same conditions on the four propellers (same cavitation number at a given advance coefficient), and at nearly the same cavitation number for all radii not covered by sheet cavitation. For the two most highly skewed propellers, cavitation occurred along the trailing edge of the back of the blade near the hub. For Propeller 4384 (skew = 108 deg), this was the first cavitation occurring in the range J = 0.95 to J = 1.2.

Comparison of the back and face sheet cavitation inception of the four propellers (see Figure 6) showed a substantial widening of the cavitation-free bucket with increasing skew. However, some crossover in the inception of the back cavitation and tip vortex cavitation occurred for the three skewed propellers such that at design advance coefficient, sheet cavitation was delayed most on Propeller 4382 (skew = 36 deg).

Figure 8 presents the thrust and torque breakdown due to cavitation of the four propellers. No systematic variation of thrust and torque breakdown with skew was apparent.

DISCUSSION

The reason for the widening of the cavitation-free bucket with increasing skew is not clear. It has been suggested[2] that this phenomenon may be somewhat analogous to the well-known swept-wing effect.[13] The two-dimensional swept wing reacts only to the component of velocity normal to the leading edge and thus the leading-edge pressure peak and the lift effectiveness decrease proportionally as the cosine of the sweep angle (for sections parallel to the flow held invariant with sweep). This analogy predicts that the propeller lift effectiveness decreases substantially with increasing skew; however, the open-water tests clearly showed that the lift effectiveness is essentially independent of skew in the range of advance coefficient where cavitation data are reported. This difference in variation of lift effectiveness suggests that the effect of propeller blade skew on cavitation inception cannot be explained by the swept-wing analogy.

It is hypothesized that the widening of the cavitation bucket with increasing skew is due to a secondary flow which tends to equalize the pressure on the face and back along the leading edge of highly skewed propellers. It is well-known that such secondary flow takes place at the blade tip. However, such a secondary flow could also take place along the leading edge, which is not perpendicular to the resultant flow,[14] such as for highly skewed propellers. Such a flow could reduce the local suction peak at the leading edge and thus delay leading-edge cavitation without measurably affecting the propeller thrust and torque.

Another possible explanation could lie in the variation with skew of induced velocities (especially near the leading edge) at off-design advance coefficient J. The variation of induced velocities with skew could produce progressively smaller pressure peaks at the leading edge with increasing skew. At the same time, the lift (and thus propeller thrust and torque) could remain essentially invariant with skew due to changes in induced velocities on regions of the blade removed from the leading edge. This hypothesis can be checked when suitable lifting-surface theories become available for accurately calculating detailed off-design propeller performance.

Prior to full-scale trial evaluation, it is not believed that the scaling problem for leading edge cavitation on skewed propellers is different from that for unskewed propellers.

CONCLUSIONS

The following conclusions are drawn from the present study:

1. The design procedure is very satisfactory for highly skewed propellers. All four propellers operated within 1 percent of design rpm in open water.

2. The cavitation-free bucket becomes substantially wider with increasing skew. However, some crossover in the inception of back cavitation and tip vortex cavitation occurred for the three skewed designs near design advance coefficient. Hence, near the self-propulsion

condition, the propeller with 36 deg of skew had the highest cavitation inception speed. Face cavitation inception speed increases monotonically with increasing skew at all advance coefficients.

3. The forward open-water propulsion characteristics including lift effectiveness and performance breakdown due to cavitation are insensitive to skew.

4. At constant power and thrust loading coefficient, the backing speed decreases slightly with increasing skew. The backing speeds with 36, 72, and 108 degrees of skew were approximately 1.5, 8.0, and 12.5 percent less respectively than the backing speed with zero skew.

ACKNOWLEDGMENTS

The assistance of Friede and Goldman, Inc. in administering the financial support under the development program for the LASH cargo vessels is acknowledged. The author is grateful to Mr. Dennis E. Crown who conducted most of the open-water tests and to Mr. Dusan Lysy for his help in the cavitation tests and data reduction.

Figure 1 – Blade Outlines of the Four Model Propellers

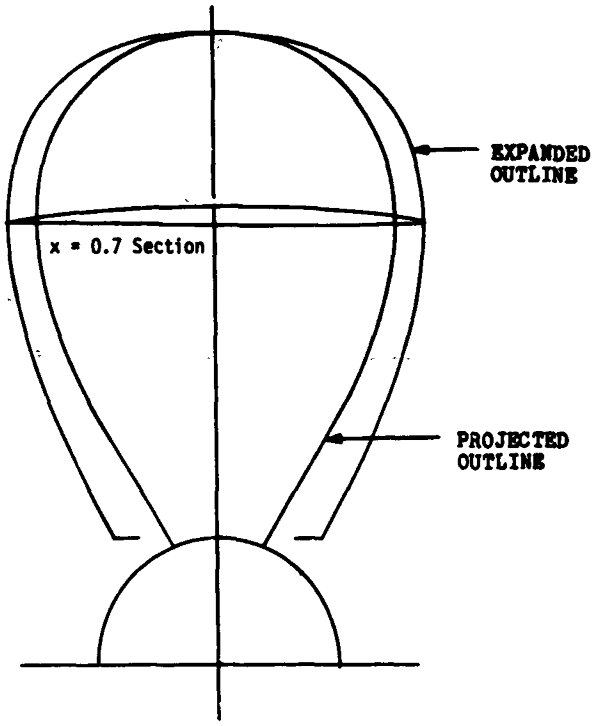

Figure 1a – Propeller 4381, Skew 0 Degree

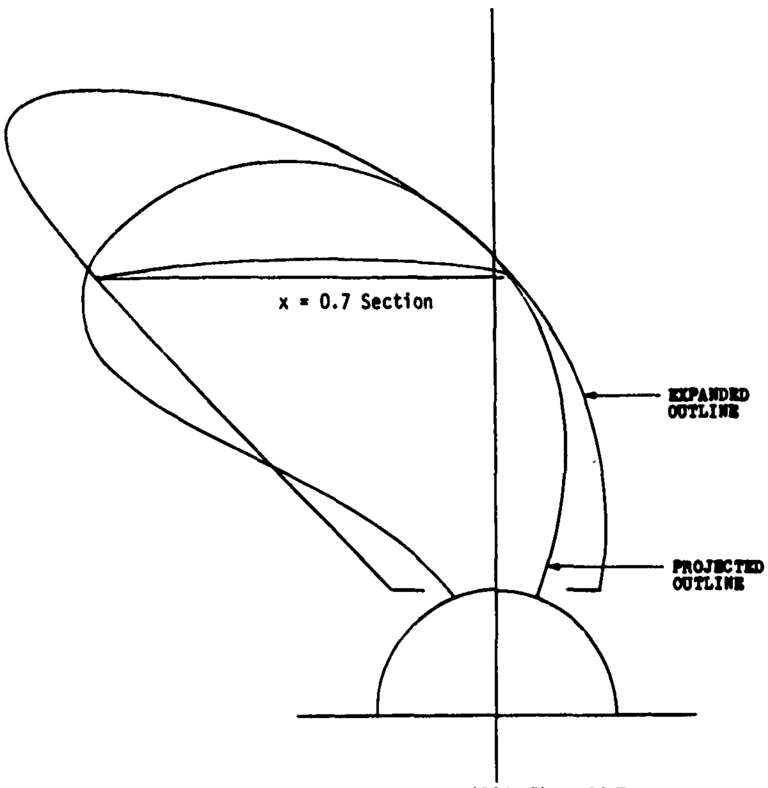

Figure 1b – Propeller 4382, Skew 36 Degrees

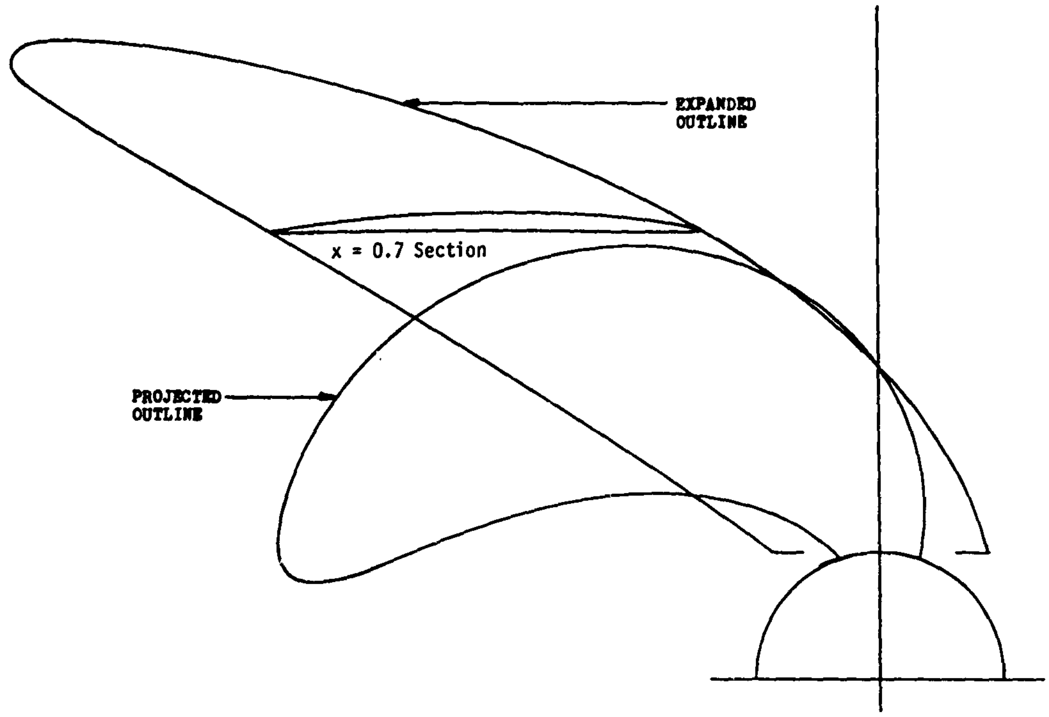

Figure 1c – Propeller 4383, Skew 72 Degrees

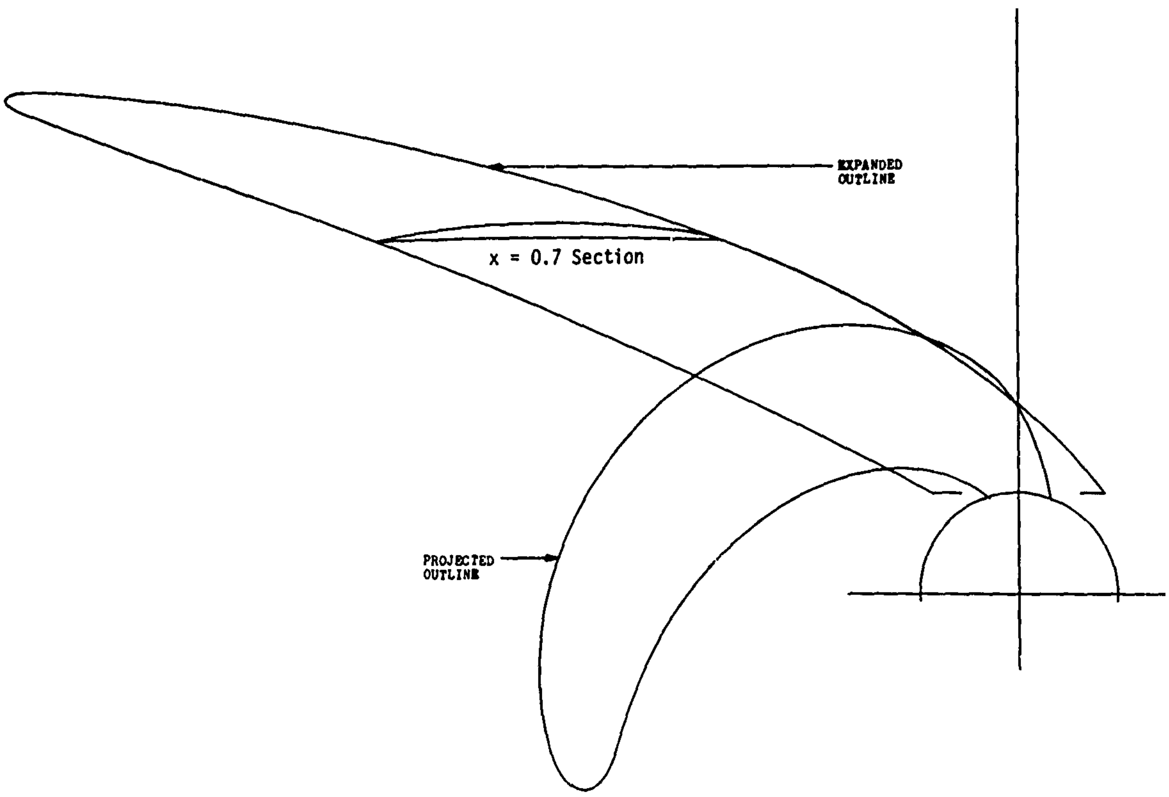

Figure 1d – Propeller 4384, Skew 108 Degrees

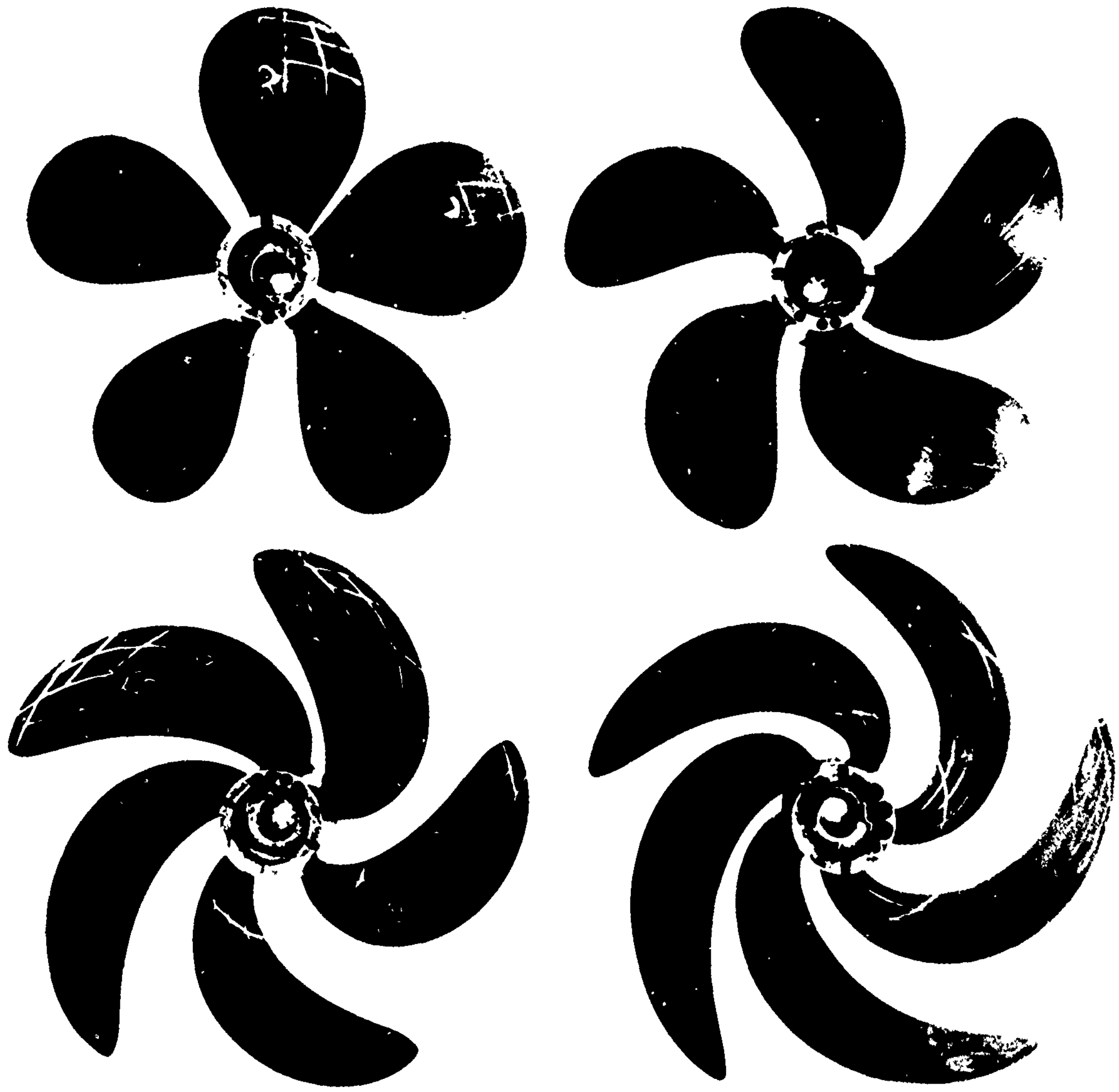

Figure 2 – Longitudinal View of the Skewed Propeller Series

Figure 3 – Forward Open-Water Characteristics of the Propellers

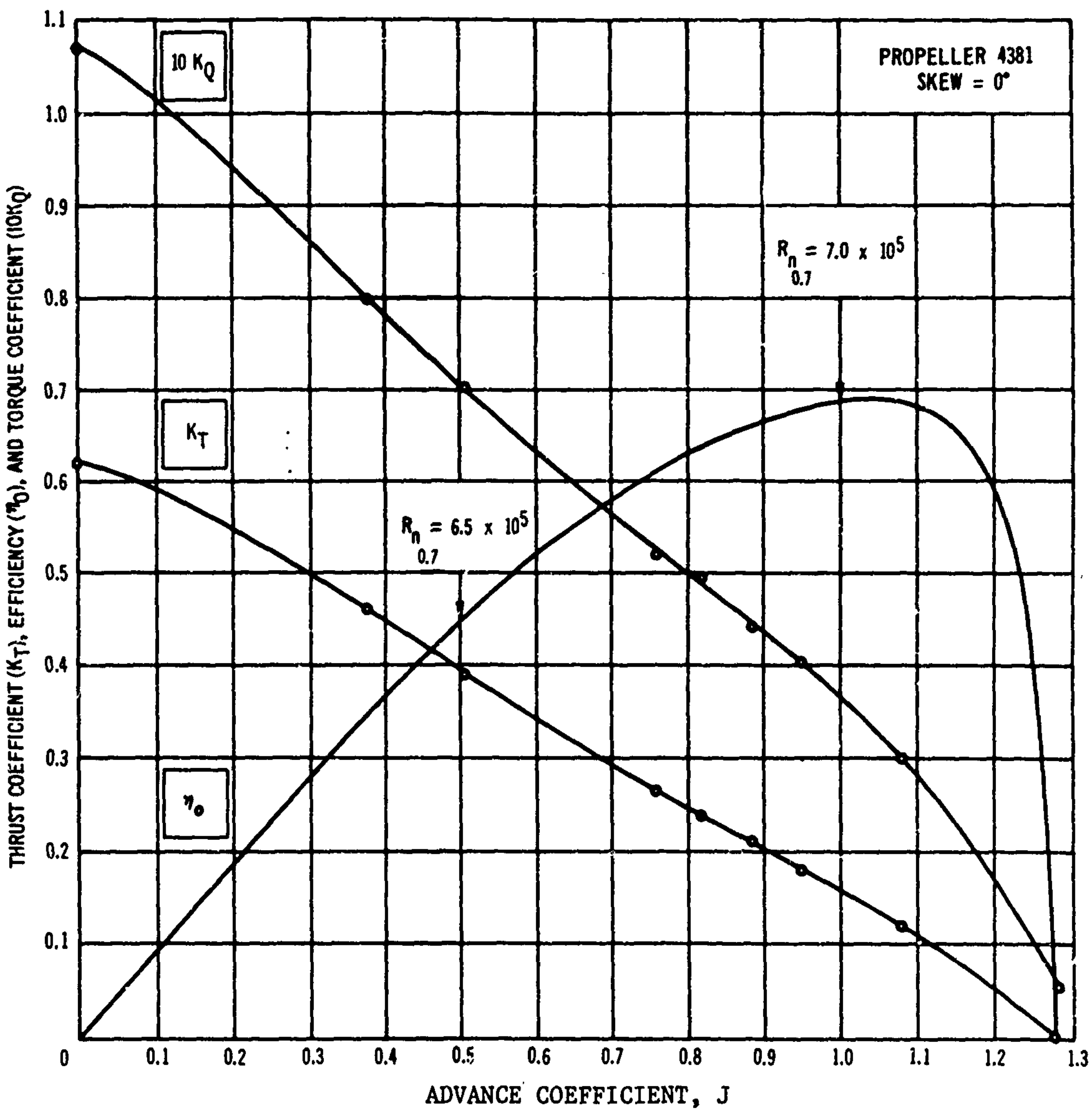

Figure 3a

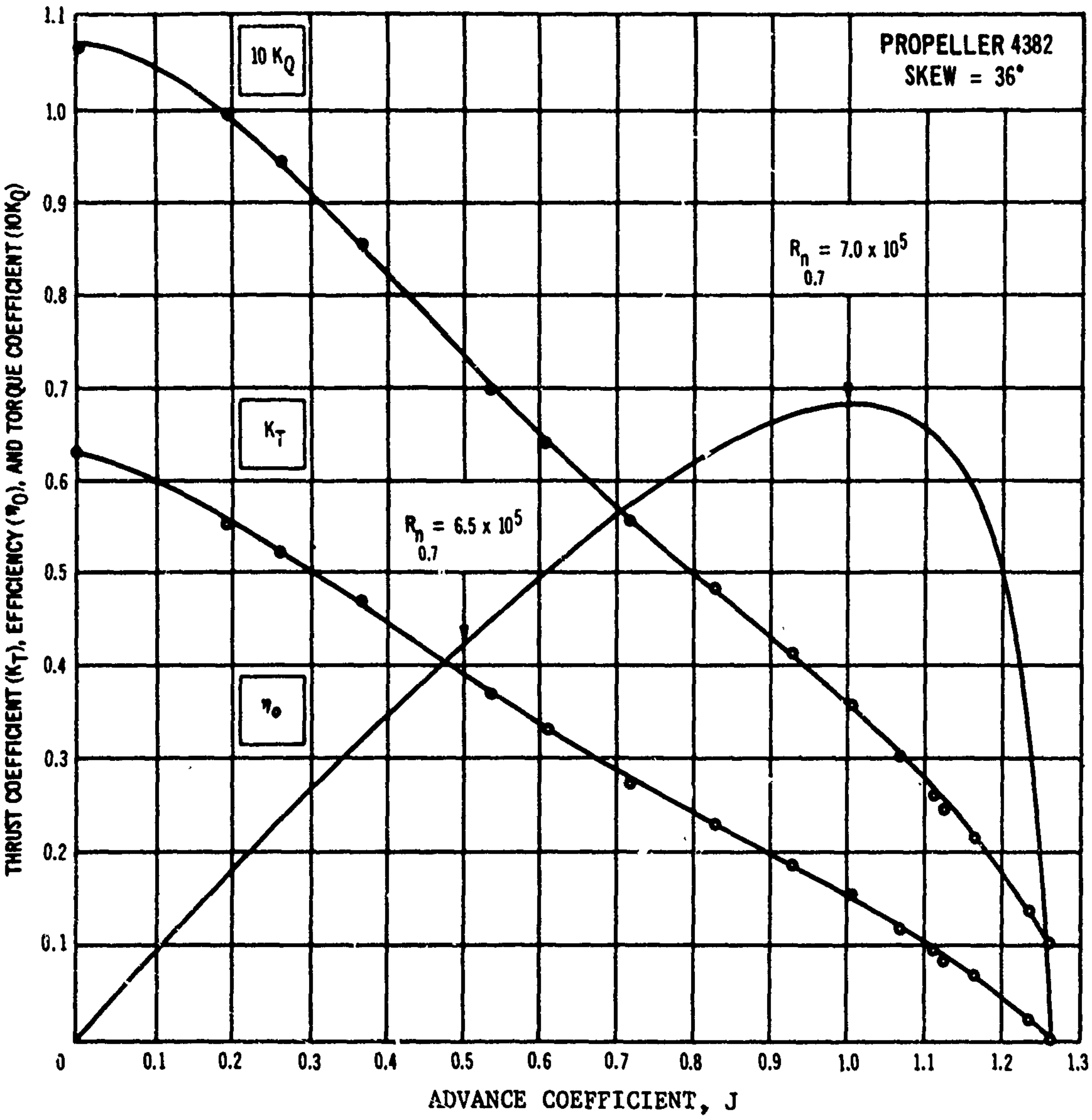

PROPELLER 4382
SKEW = 36°
10 K_Q
K_T
η_o
$R_{n_{0.7}} = 7.0 \times 10^5$
$R_{n_{0.7}} = 6.5 \times 10^5$
THRUST COEFFICIENT (K_T), EFFICIENCY (η_O), AND TORQUE COEFFICIENT ($10K_Q$)
ADVANCE COEFFICIENT, J
0
0.1
0.2
0.3
0.4
0.5
0.6
0.7
0.8
0.9
1.0
1.1
1.2
1.3

Figure 3b

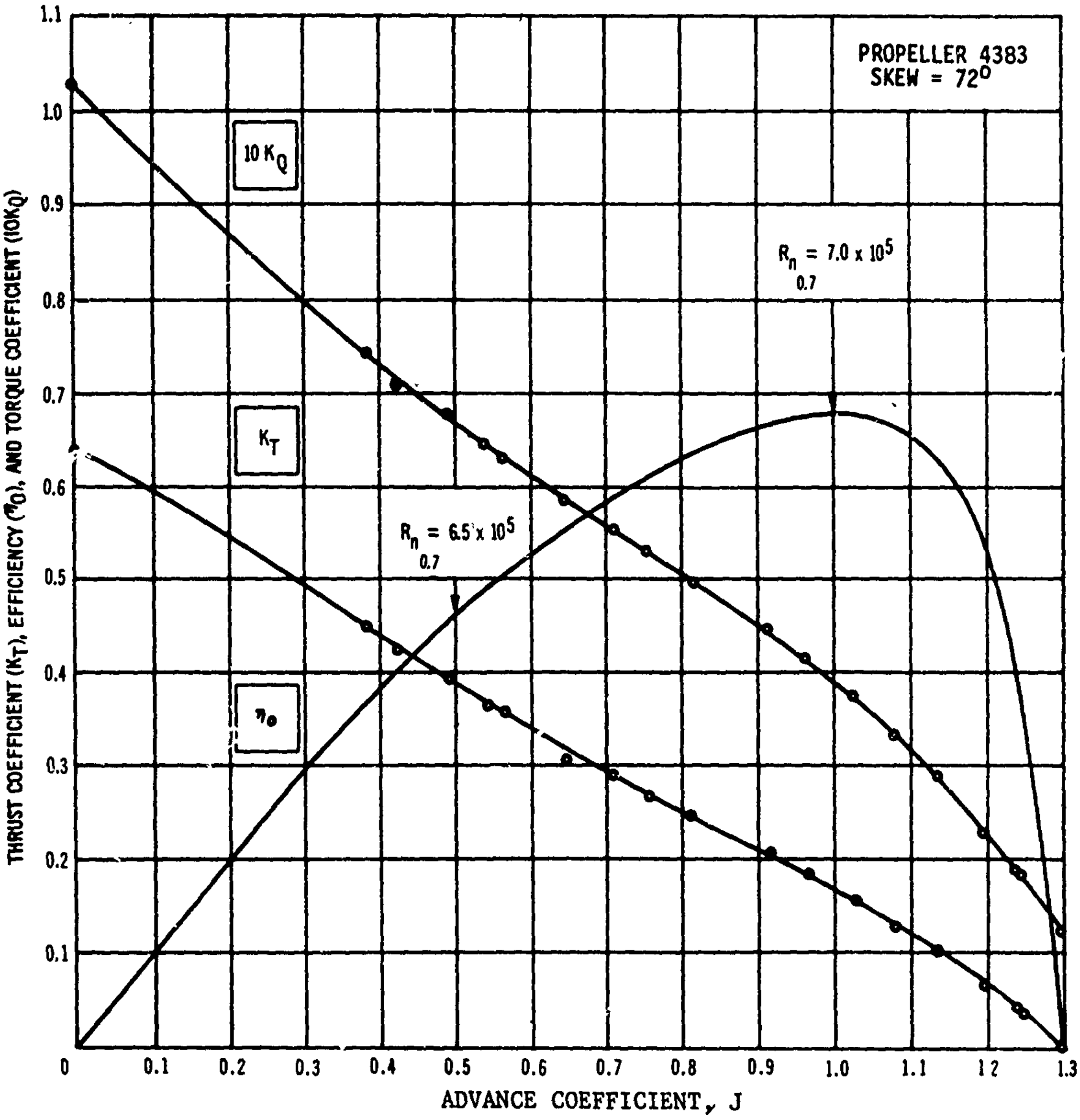
PROPELLER 4383
SKEW = 72°
10 K_Q
K_T
η_o
$R_{n_{0.7}} = 7.0 \times 10^5$
$R_{n_{0.7}} = 6.5 \times 10^5$
THRUST COEFFICIENT (K_T), EFFICIENCY (η_o), AND TORQUE COEFFICIENT ($10K_Q$)
ADVANCE COEFFICIENT, J

Figure 3c

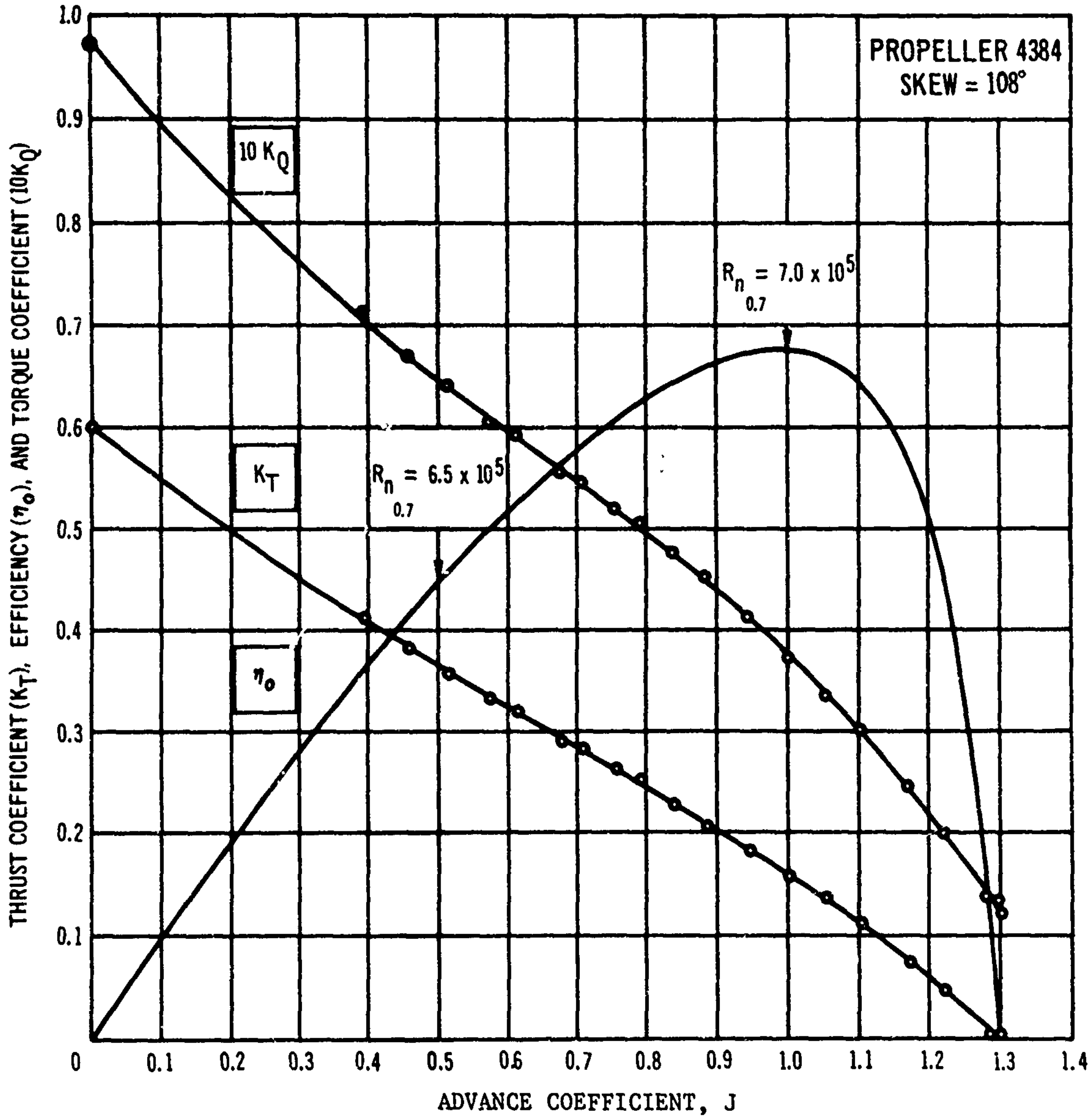
PROPELLER 4384
SKEW = 108°
10 K_Q
K_T
η_o
$R_{n_{0.7}} = 7.0 \times 10^5$
$R_{n_{0.7}} = 6.5 \times 10^5$
THRUST COEFFICIENT (K_T), EFFICIENCY (η_o), AND TORQUE COEFFICIENT ($10K_Q$)
ADVANCE COEFFICIENT, J

Figure 3d

Figure 4 – Backing Open-Water Characteristics of the Propellers

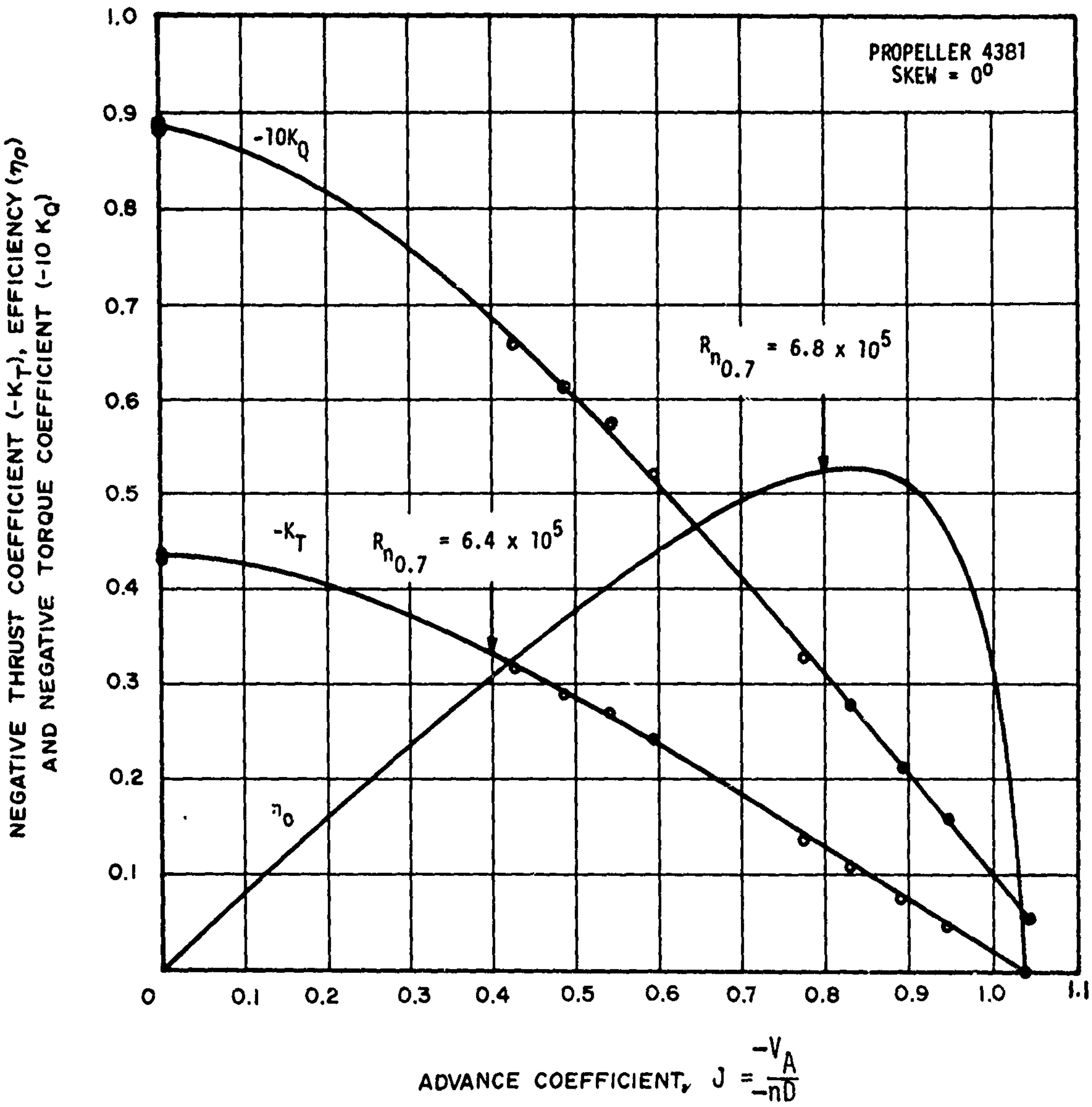

Figure 4a

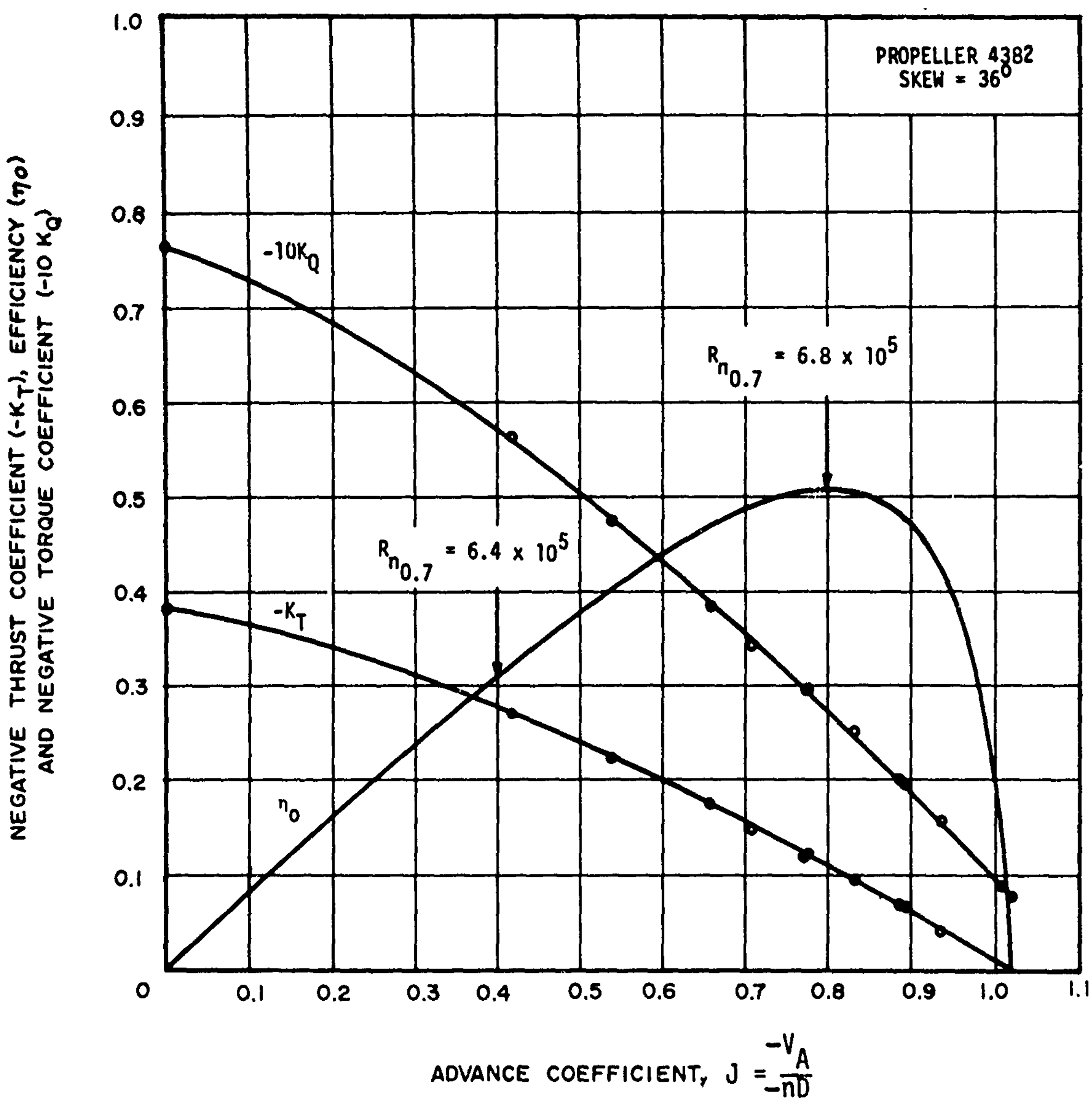
PROPELLER 4382
SKEW = 36°
-10K_Q
-K_T
η_0
R_n0.7 = 6.8 x 10^5
R_n0.7 = 6.4 x 10^5
NEGATIVE THRUST COEFFICIENT (-K_T), EFFICIENCY (η_0)
AND NEGATIVE TORQUE COEFFICIENT (-10 K_Q)
ADVANCE COEFFICIENT, J = -V_A/-nD
0 0.1 0.2 0.3 0.4 0.5 0.6 0.7 0.8 0.9 1.0 1.1

Figure 4b

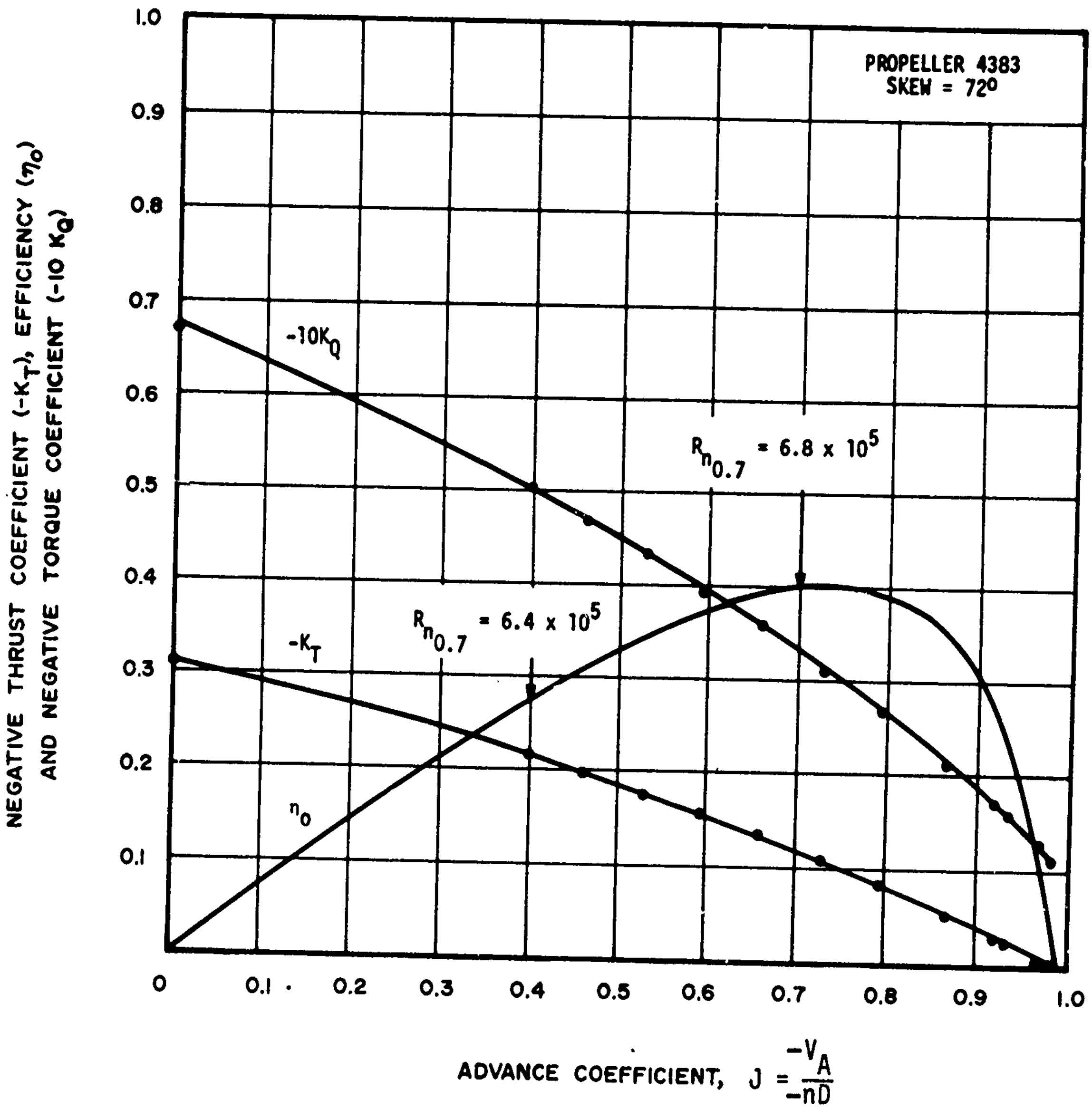

PROPELLER 4383
SKEW = 72°
-10K$_Q$
-K$_T$
η_o
$R_{n_{0.7}}$ = 6.8 x 10^5
$R_{n_{0.7}}$ = 6.4 x 10^5
1.0
0.9
0.8
0.7
0.6
0.5
0.4
0.3
0.2
0.1
0
0.1
0.2
0.3
0.4
0.5
0.6
0.7
0.8
0.9
1.0
NEGATIVE THRUST COEFFICIENT (-K$_T$), EFFICIENCY (η_o)
AND NEGATIVE TORQUE COEFFICIENT (-10 K$_Q$)
ADVANCE COEFFICIENT, J = $\frac{-V_A}{-nD}$

Figure 4c

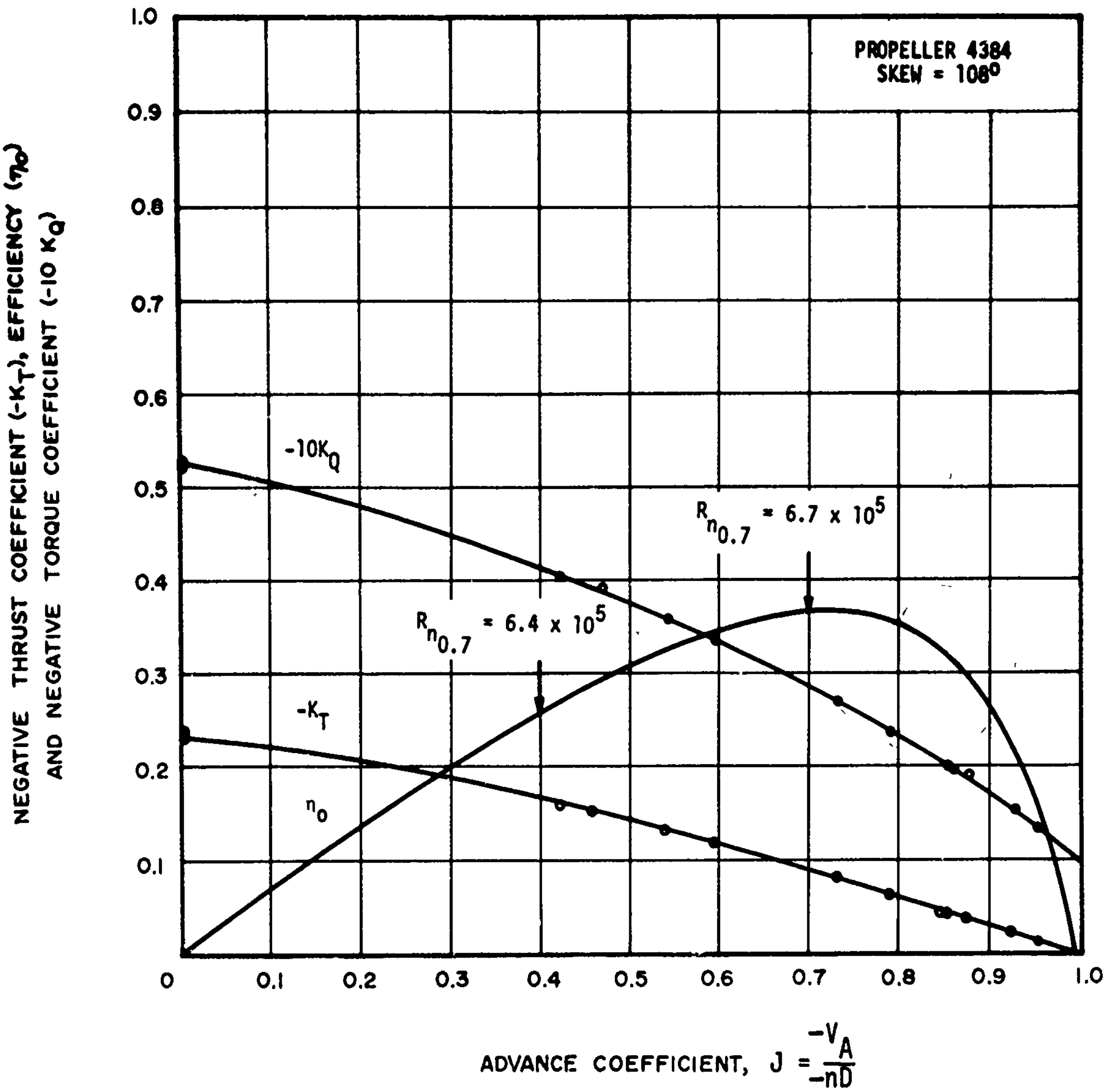

PROPELLER 4384
SKEW = 108°
-10K_Q
-K_T
n_o
R_n0.7 = 6.4 x 10^5
R_n0.7 = 6.7 x 10^5
NEGATIVE THRUST COEFFICIENT (-K_T), EFFICIENCY (η_o)
AND NEGATIVE TORQUE COEFFICIENT (-10 K_Q)
ADVANCE COEFFICIENT, J = -V_A/-nD
0
0.1
0.2
0.3
0.4
0.5
0.6
0.7
0.8
0.9
1.0

Figure 4d

Figure 5 – Cavitation Inception on the Propellers at Various Radii

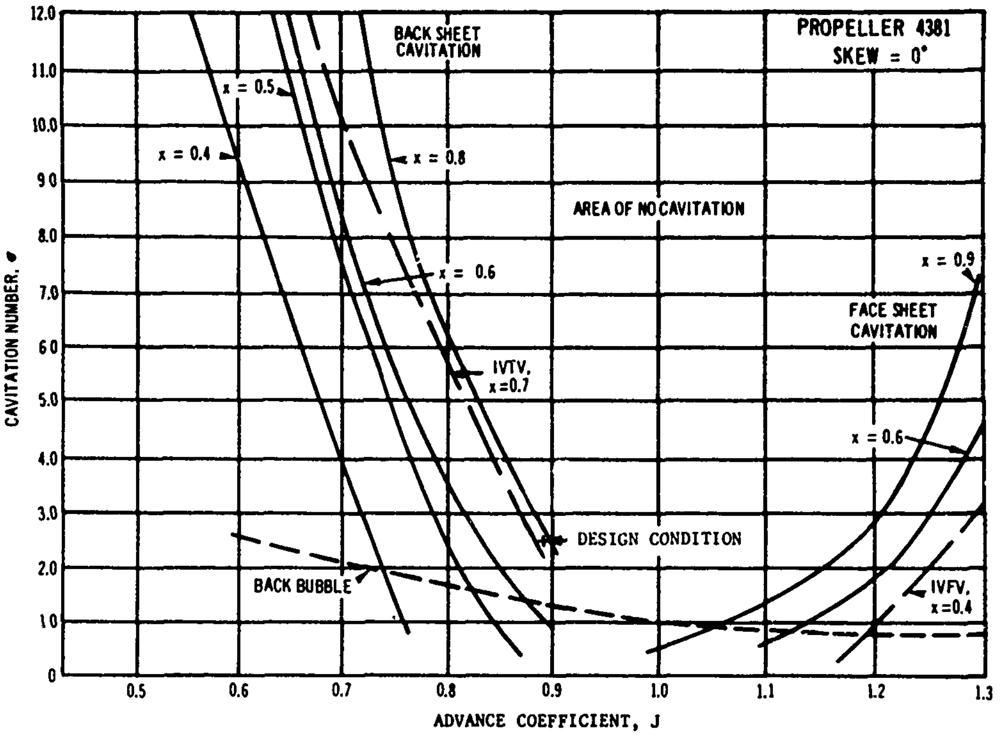

Figure 5a

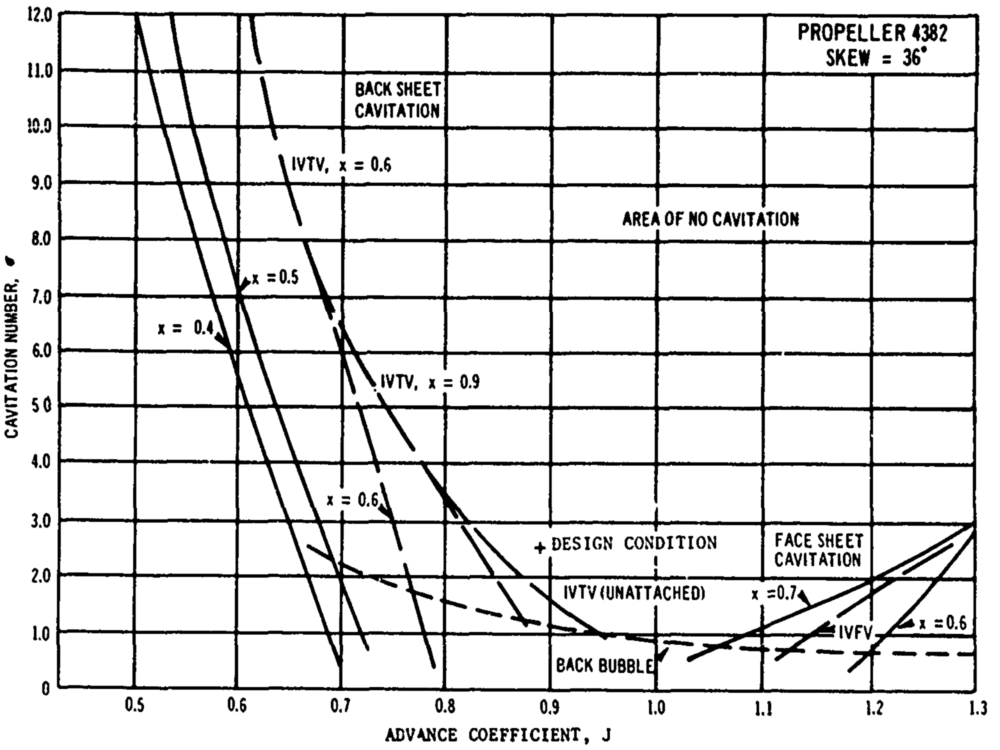

Figure 5b

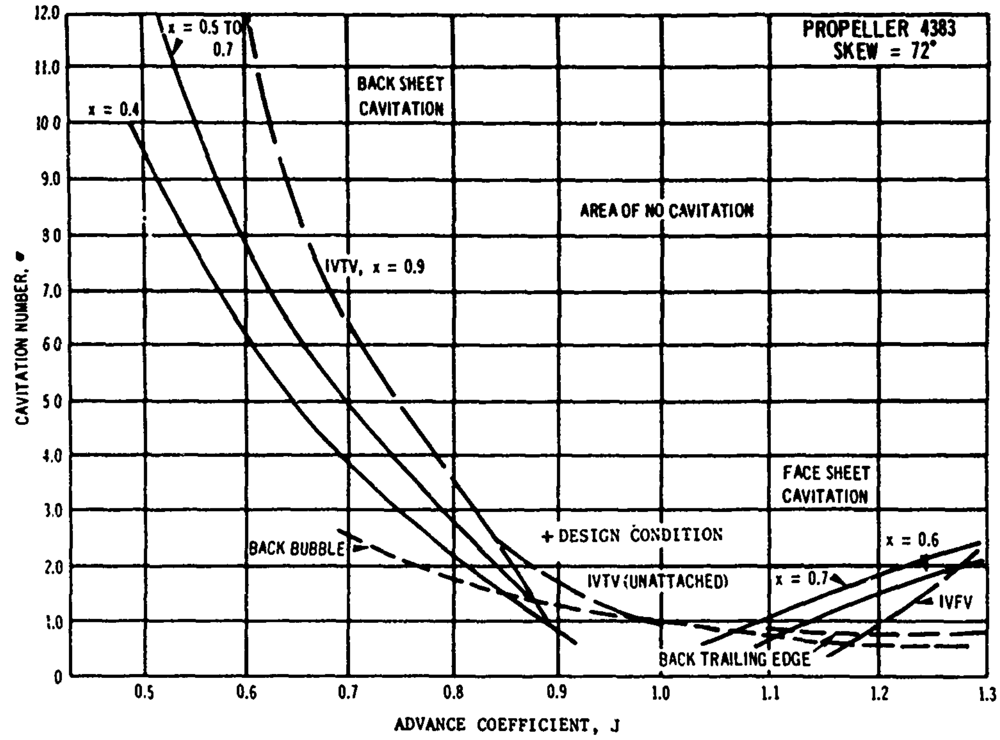

Figure 5c

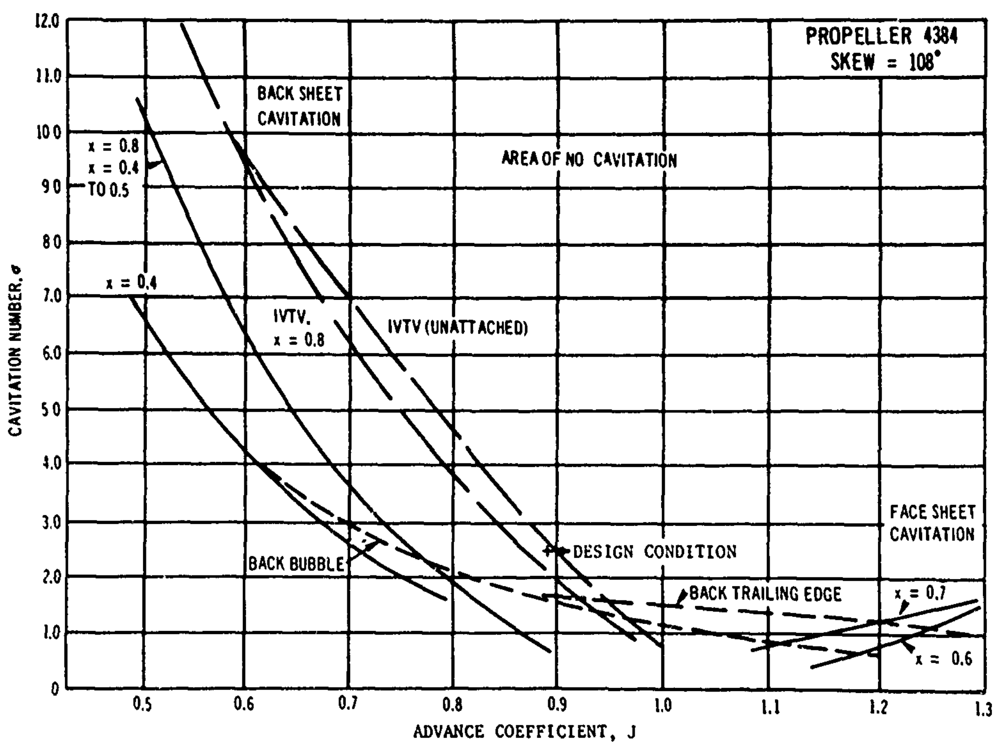

Figure 5d

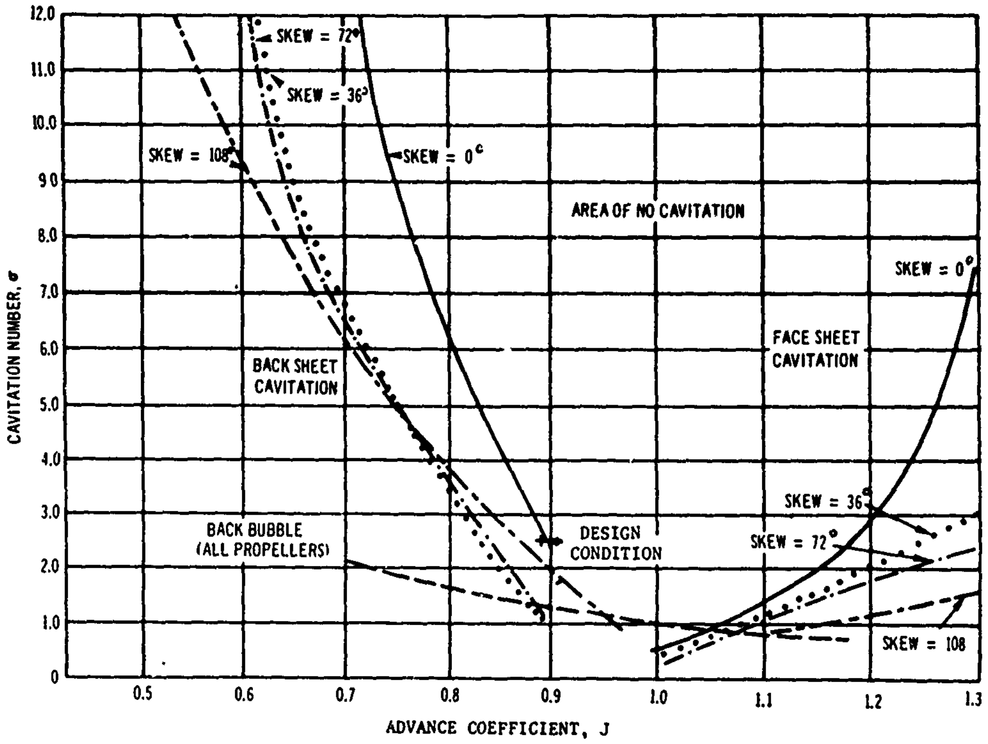

Figure 6 – Comparison of Cavitation Inception on the Different Propellers

Figure 7 – Illustrations of Cavitation at Selected Advance Coefficients J and Cavitation Numbers σ

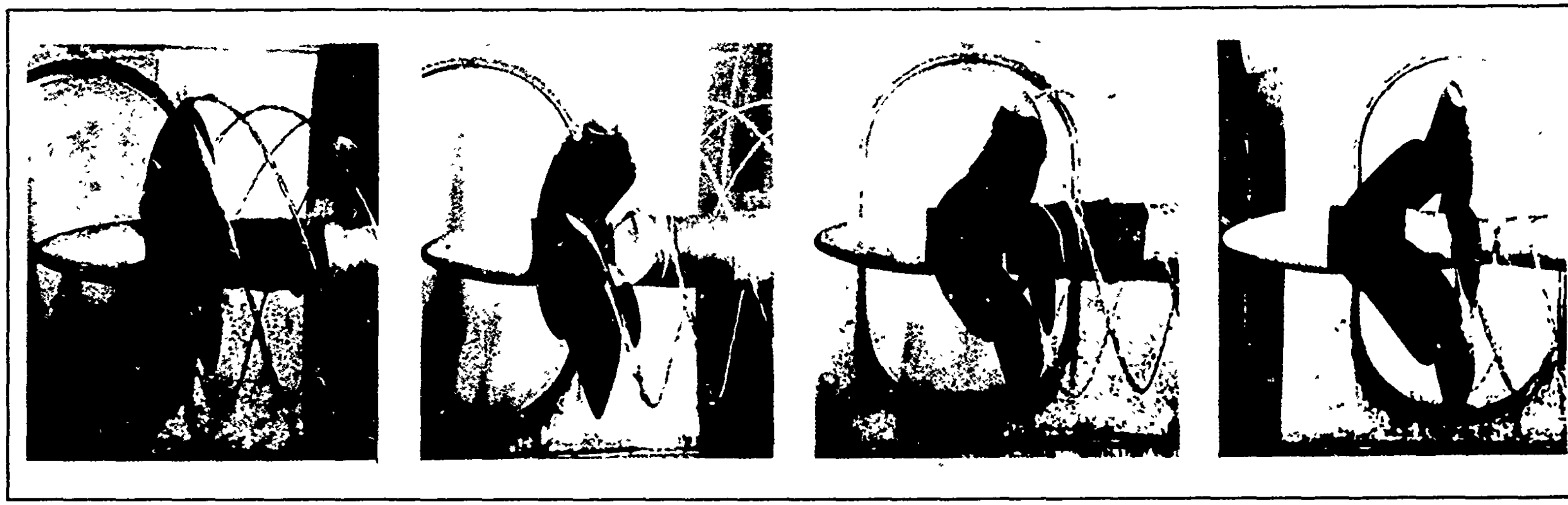

Skew = 0 Degrees | Skew = 36 Degrees | Skew = 72 Degrees | Skew = 108 Degrees

NOT REPRODUCIBLE

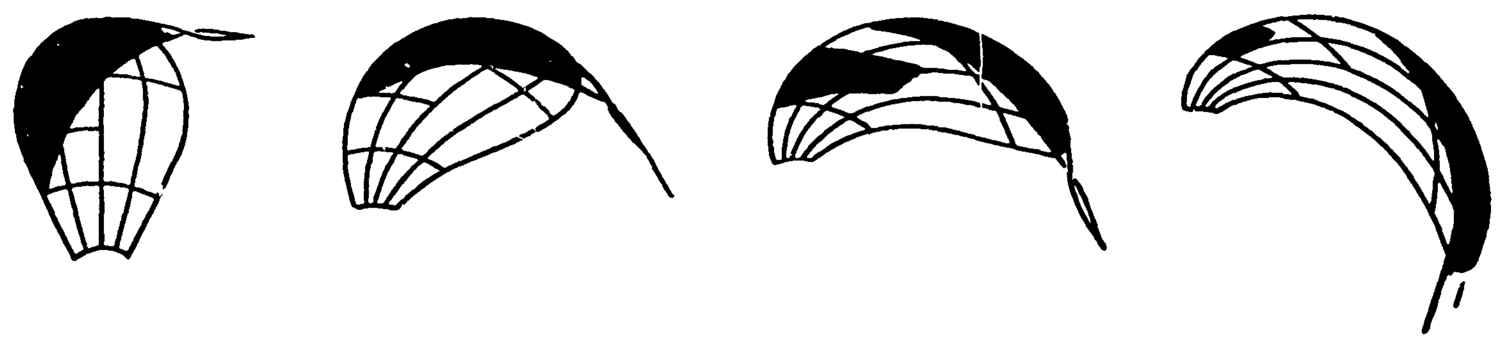

Figure 7a – $J = 0.7$, $\sigma = 3.5$
(sketches show back cavitation)

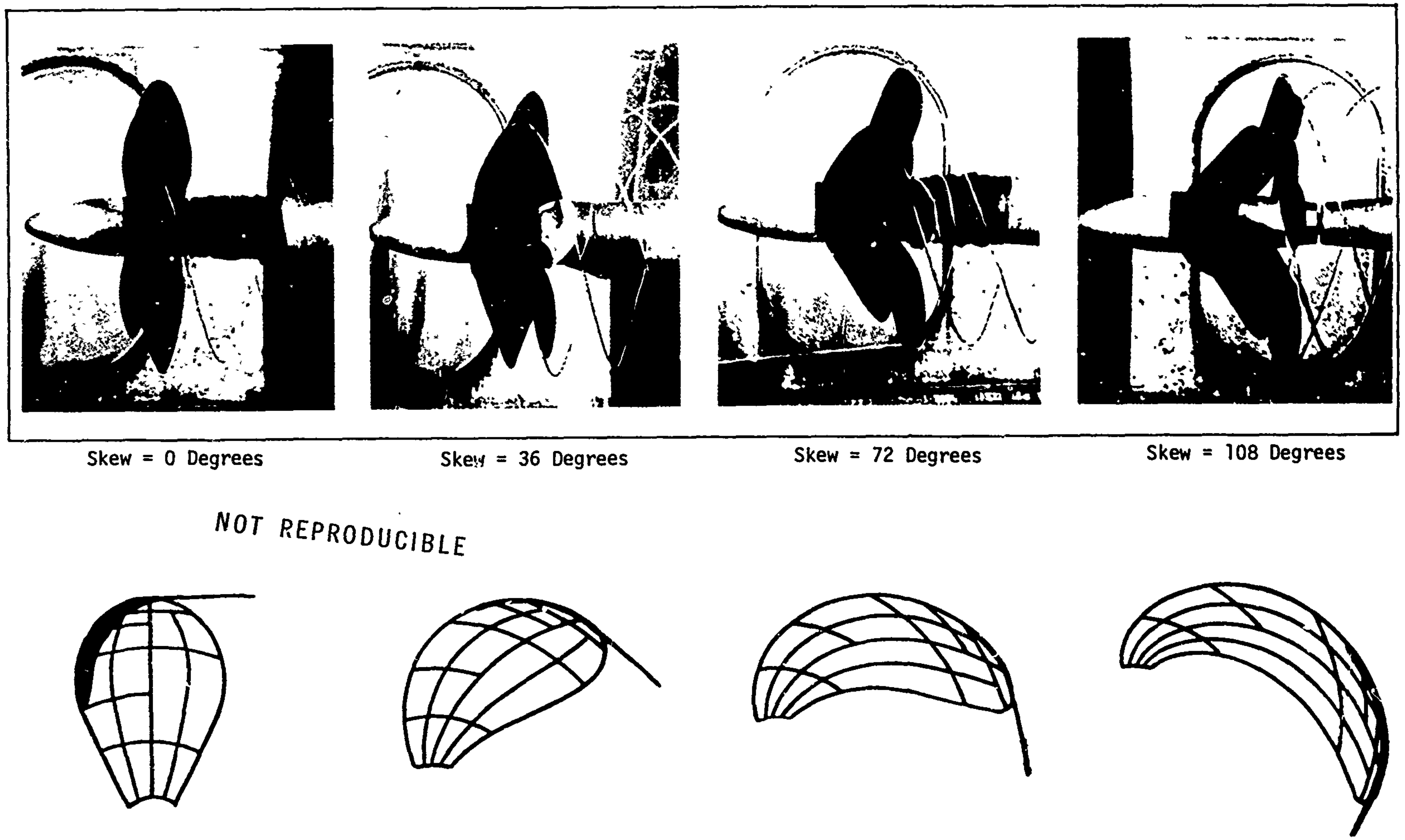

Figure 7b – $J = 0.8$, $\sigma = 3.5$
(sketches show back cavitation)

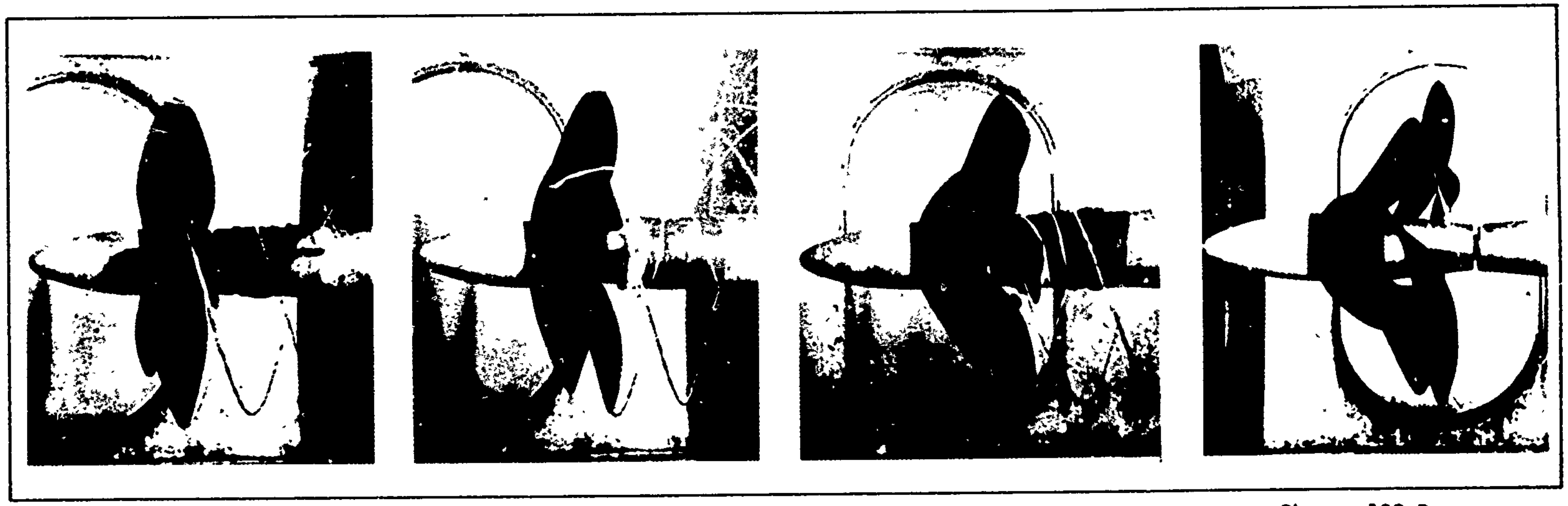

Skew = 0 Degrees | Skew = 36 Degrees | Skew = 72 Degrees | Skew = 108 Degrees

NOT REPRODUCIBLE

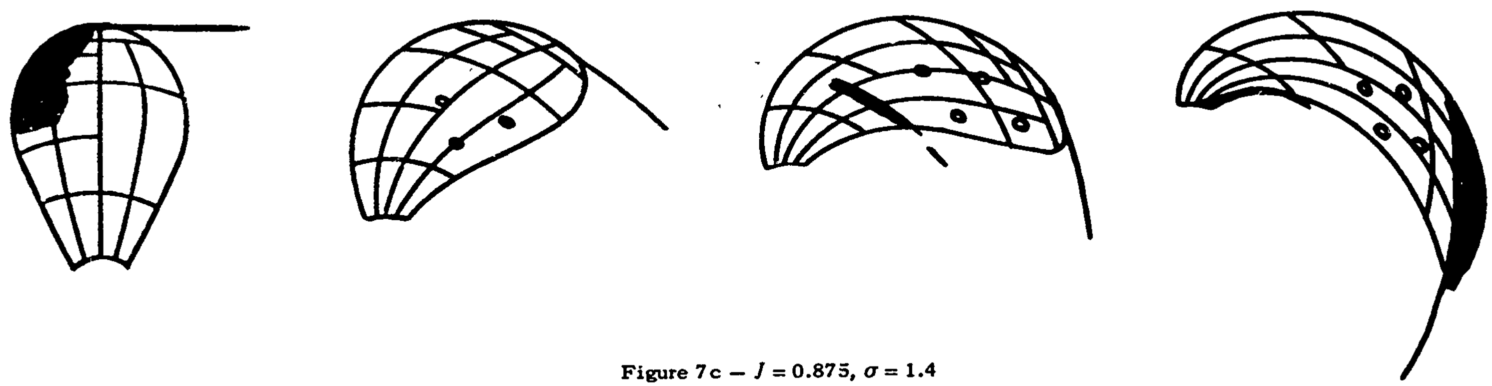

Figure 7c — $J = 0.875$, $\sigma = 1.4$
(sketches show back cavitation)

Skew = 36 Degrees

Skew = 108 Degrees

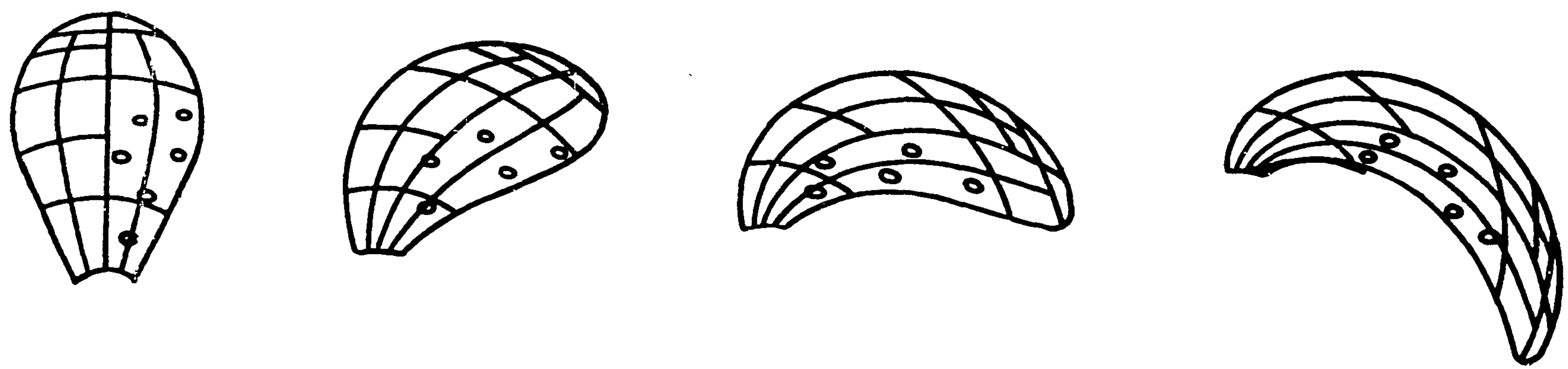

Figure 7d — $J = 1.0$, $\sigma = 0.9$
(sketches show back cavitation)

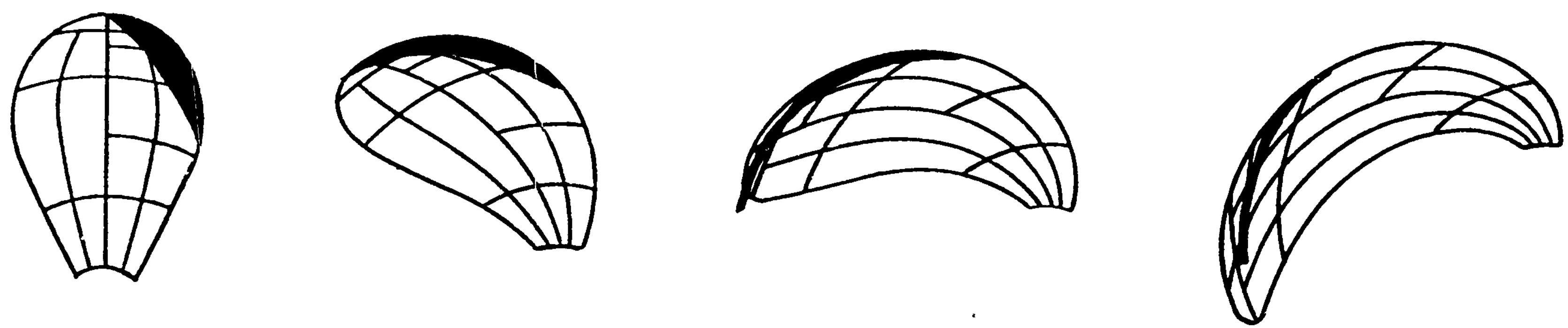

Figure 7e — $J = 1.1$, $\sigma = 0.8$
(sketches show face cavitation)

Skew = 36 Degrees

Skew = 72 Degrees

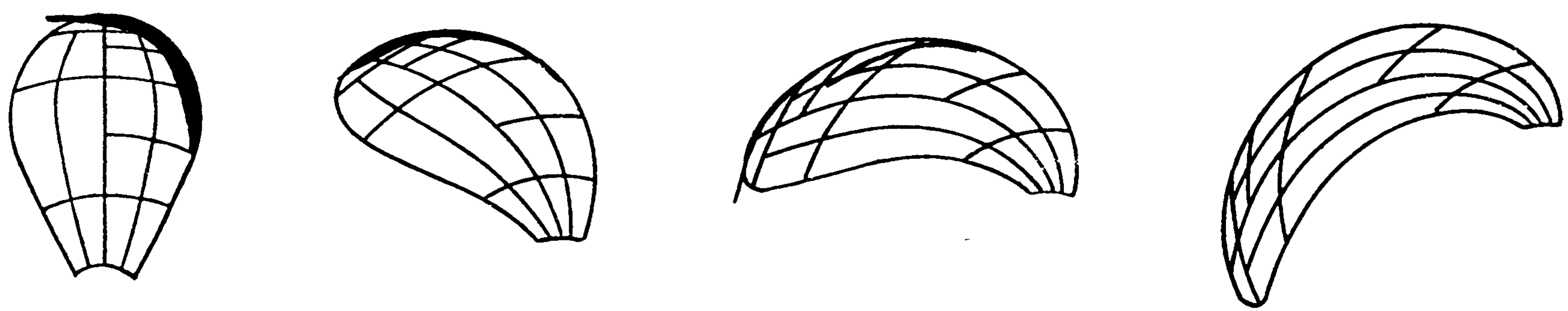

Figure 7f – $J = 1.2$, $\sigma = 1.7$
(sketches show face cavitation)

Figure 8 – Thrust and Torque Breakdown Due to Cavitation on the Propellers

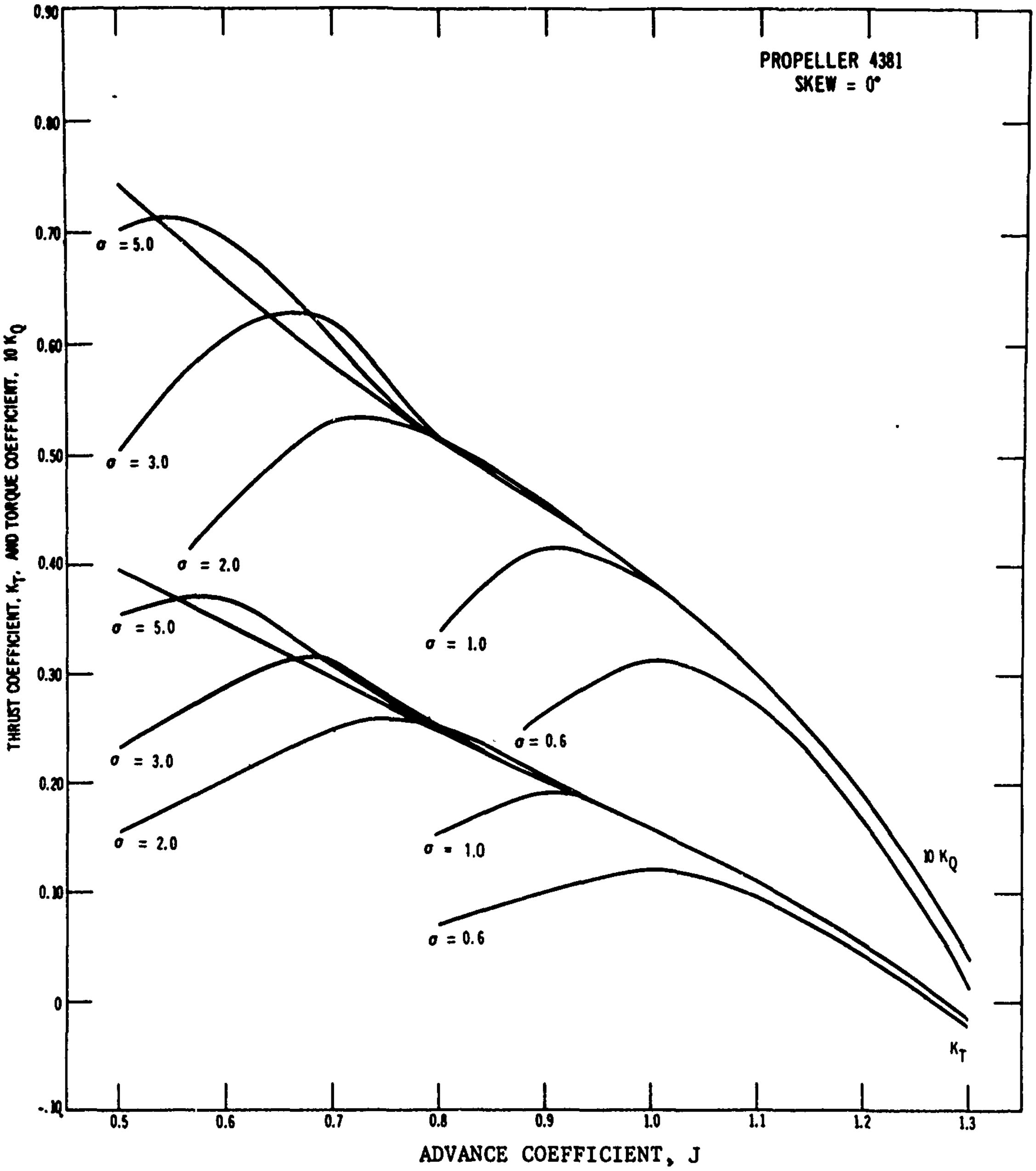

Figure 8a

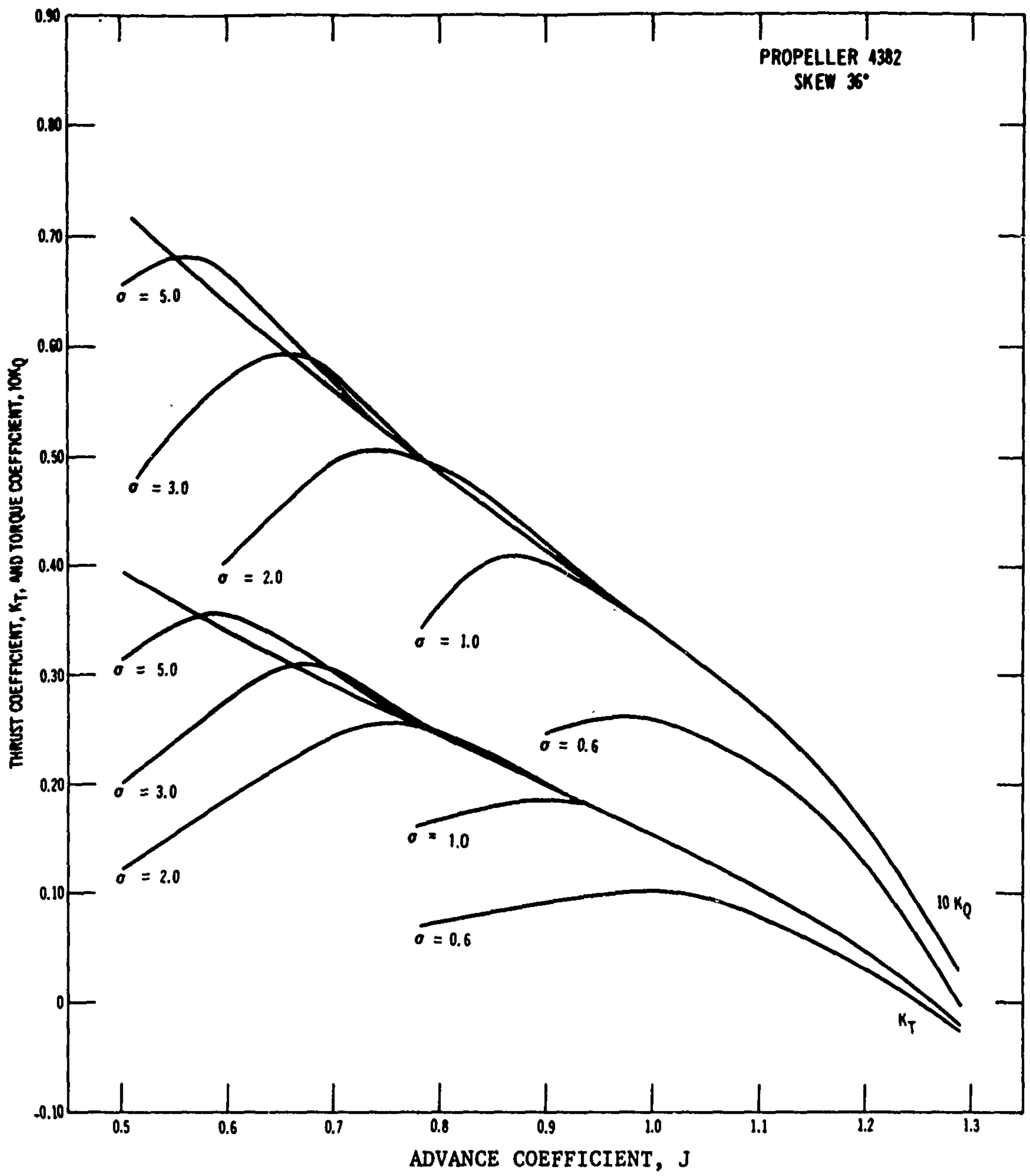
PROPELLER 4382
SKEW 36°
THRUST COEFFICIENT, K_T, AND TORQUE COEFFICIENT, $10K_Q$
ADVANCE COEFFICIENT, J
σ = 5.0
σ = 3.0
σ = 2.0
σ = 1.0
σ = 0.6
σ = 5.0
σ = 3.0
σ = 2.0
σ = 1.0
σ = 0.6
10 K_Q
K_T
0.90
0.80
0.70
0.60
0.50
0.40
0.30
0.20
0.10
0
-0.10
0.5
0.6
0.7
0.8
0.9
1.0
1.1
1.2
1.3

Figure 8b

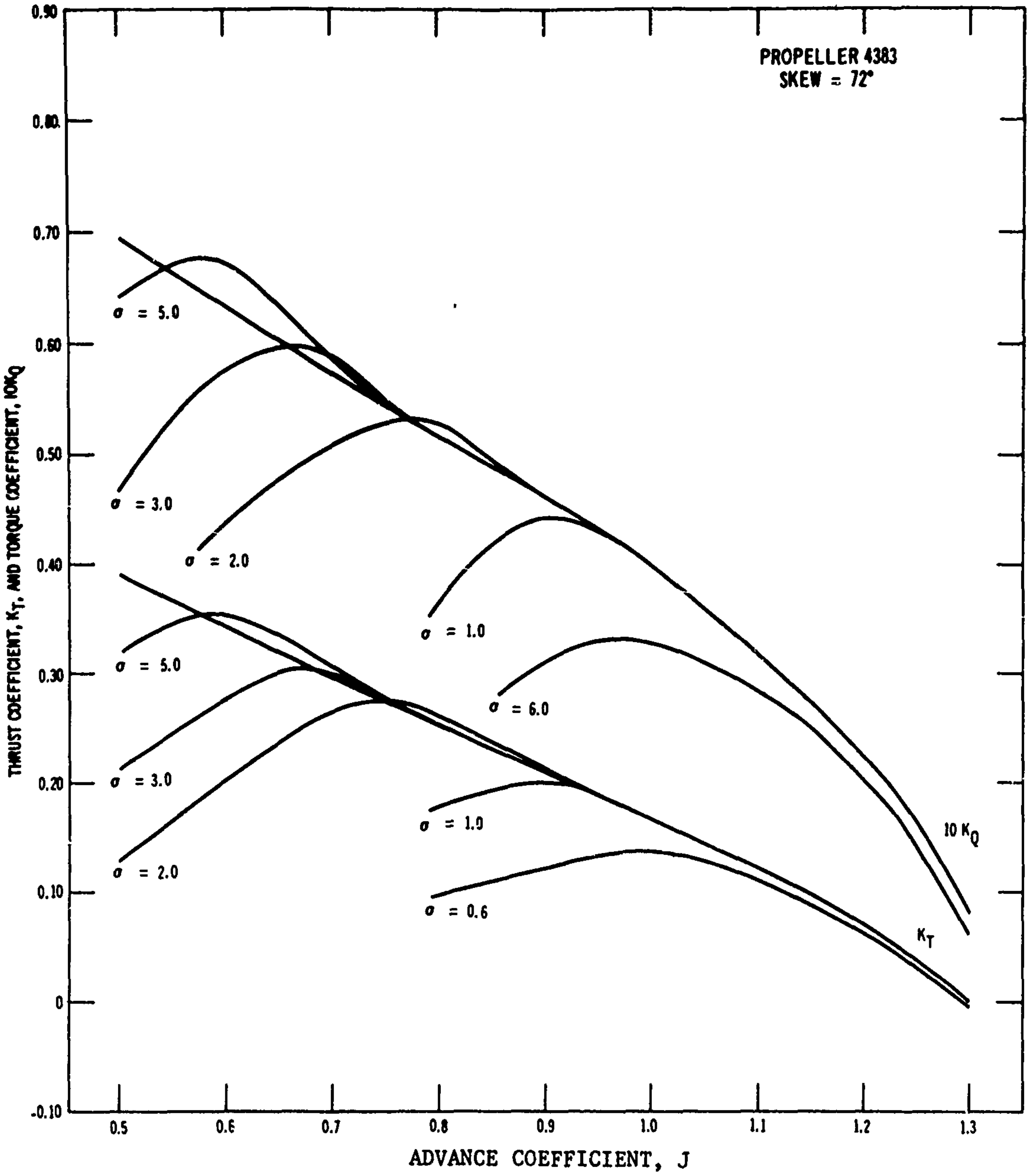

PROPELLER 4383
SKEW = 72°
THRUST COEFFICIENT, K_T, AND TORQUE COEFFICIENT, $10K_Q$
ADVANCE COEFFICIENT, J
σ = 5.0
σ = 3.0
σ = 2.0
σ = 1.0
σ = 6.0
σ = 5.0
σ = 3.0
σ = 1.0
σ = 2.0
σ = 0.6
10 K_Q
K_T
0.90
0.80
0.70
0.60
0.50
0.40
0.30
0.20
0.10
0
-0.10
0.5
0.6
0.7
0.8
0.9
1.0
1.1
1.2
1.3

Figure 8c

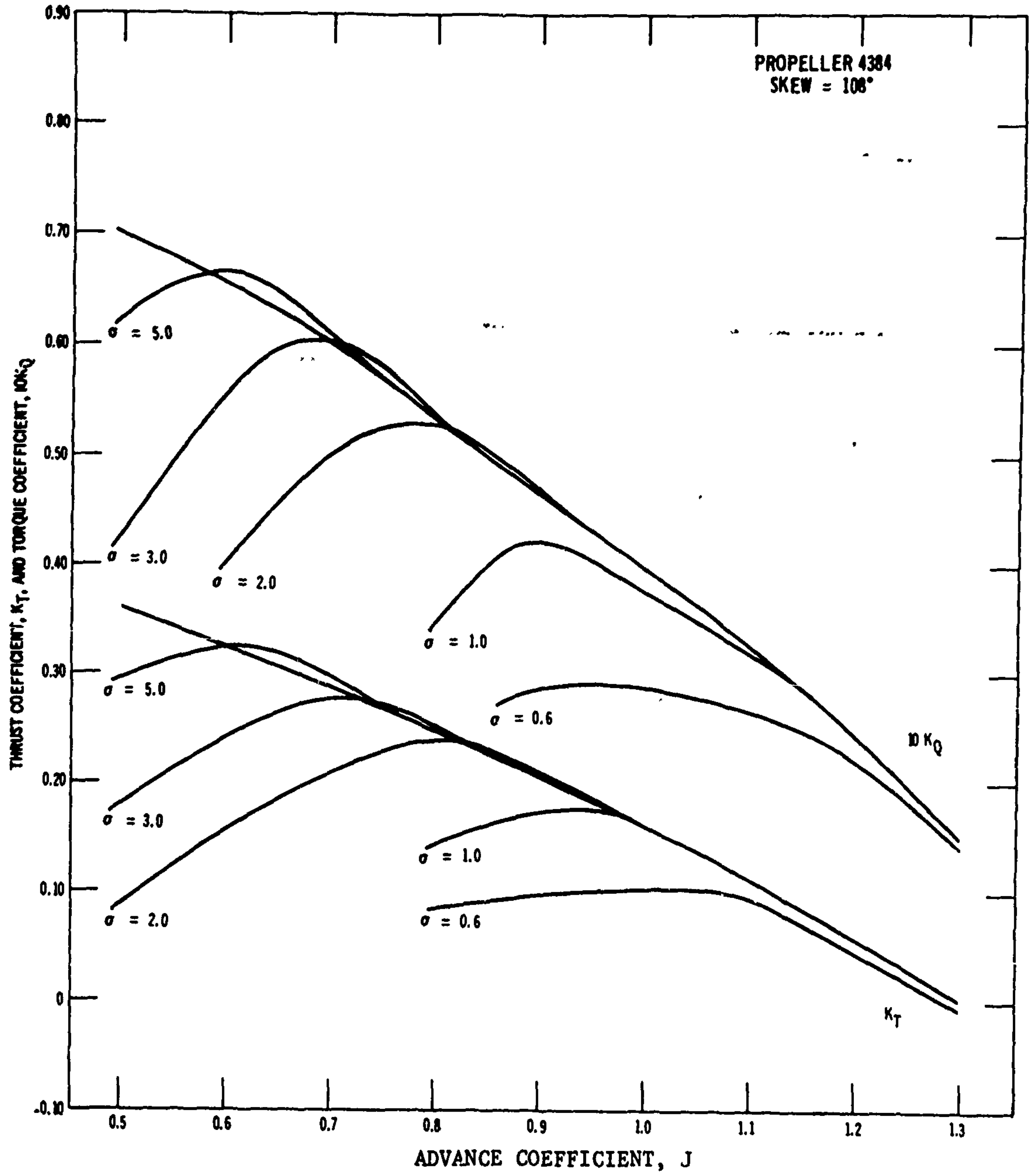
PROPELLER 4384
SKEW = 108°
THRUST COEFFICIENT, K_T, AND TORQUE COEFFICIENT, $10K_Q$
ADVANCE COEFFICIENT, J
$10\ K_Q$
K_T
σ = 5.0
σ = 3.0
σ = 2.0
σ = 1.0
σ = 0.6

Figure 8d

REFERENCES

1. Boswell, R.J. and Miller, M.L., "Unsteady Propeller Loading - Measurement, Correlation with Theory, and Parametric Study," NSRDC Report 2625 (Oct 1968).

2. Denny, S.B., "Cavitation and Open-Water Performance of a Series of Propellers Designed by Lifting-Surface Methods," NSRDC Report 2878 (Sep 1968).

[redacted]

4. Teel, S.S. and Denny, S.B., "Field Point Pressures in the Vicinity of a Series of Skewed Marine Propellers," NSRDC Report 3278 (Aug 1970).

[redacted]

6. Shiba, H., "Air Drawing of Marine Propellers," The Transportation Technical Research Institute, Tokyo, Japan, Report 9 (1954).

7. Delano, J.B. and Harrison, D.E., "Investigation of the NACA 4-(4) (06)-057-45A and NACA 4-(4) (06)-057-45B Two-Blade Swept Propellers at Forward Mach Numbers to 0.925," NACA RM L9L05 (1950).

8. Cheng, H.M., "Hydrodynamic Aspect of Propeller Design Based on Lifting-Surface Theory, Part II - Arbitrary Chordwise Load Distribution," David Taylor Model Basin Report 1803 (Jun 1965).

9. Kerwin, J.E. and Leopold, R., "A Design Theory for Subcavitating Propellers," SNAME Vol. 72 (1964).

10. Schoenherr, K.E., "Formulation of Propeller Blade Strength," Paper presented at the Spring Meeting of SNAME (Apr 1963).

11. "Rules for Classification and Construction of Steel Vessels," American Bureau of Shipping (1964).

12. Boswell, Robert J., "Static Stress Measurements on a Highly Skewed Propeller Blade," NSRDC Report 3247 (Dec 1969).

13. Thwaites, B. (editor), "Incompressible Aerodynamics," Clarendon Press, Oxford (1960).

14. Pien, P.C., "The Calculation of Marine Propellers Based on Lifting-Surface Theory," J. Ship Res, Vol. 5, No. 2 (Sep 1961).